ELEMENTA Science of the Anthropocene

Graff, JR, et al. 2023. Reconciliation of total particulate organic carbon and nitrogen measurements determined using contrasting methods in the North Pacific Ocean as part of the NASA EXPORTS field campaign. *Elem Sci Anth*, 11: 1. DOI: https://doi.org/10.1525/elementa.2022.00112

RESEARCH ARTICLE

# Reconciliation of total particulate organic carbon and nitrogen measurements determined using contrasting methods in the North Pacific Ocean as part of the NASA EXPORTS field campaign

Jason R. Graff[1,*], Norman B. Nelson[2], Montserrat Roca-Martí[3,4], Elisa Romanelli[2], Sasha J. Kramer[2], Zach Erickson[5], Ivona Cetinić[6,7], Ken O. Buesseler[4], Uta Passow[2,8], Xiaodong Zhang[9], Claudia Benitez-Nelson[10], Kelsey Bisson[1], Hilary G. Close[11], Taylor Crockford[12], James Fox[13], Stuart Halewood[2], Phoebe Lam[14], Collin Roesler[15], Julia Sweet[16], Brian VerWey[1], Yuanheng Xiong[9], and David A. Siegel[2]

Measurements of particulate organic carbon (POC) are critical for understanding the ocean carbon cycle, including biogenic particle formation and removal processes, and for constraining models of carbon cycling at local, regional, and global scales. Despite the importance and ubiquity of POC measurements, discrepancies in methods across platforms and users, necessary to accommodate a multitude of needs and logistical constraints, commonly result in disparate results. Considerations of filter type and pore size, sample volume, collection method, and contamination sources underscore the potential for dissimilar measurements of the same variable assessed using similar and different approaches. During the NASA EXport Processes in the Ocean from RemoTe Sensing (EXPORTS) 2018 field campaign in the North Pacific Ocean, multiple methodologies and sampling approaches for determining POC were applied, including surface inline flow-through systems and depth profiles using Niskin bottles, in situ pumps, and Marine Snow Catchers. A comparison of results from each approach and platform often resulted in significant differences. Supporting measurements, however, provided the means to normalize results across datasets. Using knowledge of contrasting protocols and synchronous or near-synchronous measurements of associated environmental variables, we were able to reconcile dataset differences to account for undersampling of some particle types and sizes, possible sample contamination and blank corrections. These efforts resulted in measurement agreement between initially contrasting datasets and insights on long-acknowledged but rarely resolved discrepancies among contrasting methods for assessing POC concentrations in the ocean.

**Keywords:** Particulate organic carbon and nitrogen, High-performance liquid chromatography, Phytoplankton pigments, Particle size distribution, Particulate beam attenuation, Particulate backscattering

[1] Department of Botany & Plant Pathology, Oregon State University, Corvallis, OR, USA

[2] Earth Research Institute, University of California, Santa Barbara, CA, USA

[3] Department of Oceanography, Dalhousie University, Halifax, NS, Canada

[4] Department of Marine Chemistry & Geochemistry, Woods Hole Oceanographic Institution, Woods Hole, MA, USA

[5] NOAA/Pacific Marine Environmental Laboratory, Seattle, WA, USA

[6] Ocean Ecology Laboratory, NASA Goddard Space Flight Center, Greenbelt, MD, USA

[7] GESTAR II Morgan State University, Baltimore, MD, USA

[8] Department of Ocean Sciences, Memorial University Newfoundland, St John's, NL, Canada

[9] Division of Marine Science, School of Ocean Science and Engineering, The University of Southern Mississippi, Stennis Space Center, MS, USA

[10] School of the Earth, Ocean, and Environment, University of South Carolina, Columbia, SC, USA

[11] Rosenstiel School of Marine, Atmospheric, and Earth Science, University of Miami, Miami, FL, USA

[12] Woods Hole Oceanographic Institution, Woods Hole, MA, USA

[13] Department of Microbiology, Oregon State University, Corvallis, OR, USA

[14] Institute of Marine Sciences, University of California Santa Cruz, Santa Cruz, CA, USA

[15] Department of Earth and Oceanographic Science, Bowdoin College, Brunswick, ME, USA

[16] Department of Biology, University of Louisiana at Lafayette, Lafayette, LA, USA

* Corresponding author:
Email: graffja@oregonstate.edu

## 1. Introduction

Total particulate organic carbon (POC) in aquatic marine systems refers to both the living and non-living organic carbon associated with particles that can be separated from dissolved forms, typically through filtration techniques, and has been shown to vary in accordance with biological and environmental conditions. Surface ocean POC concentrations generally follow patterns in net primary production (NPP) with higher values found in temperate and high latitude oceans (Gardner et al., 2006). The seasonality of these regions leads to highly variable POC concentrations, with lower values typically found in winter months and maxima associated with phytoplankton blooms in spring and summer months. Conversely, the lowest surface ocean POC concentrations are found in the less productive subtropical oligotrophic gyres. POC in the open ocean is a measurement that reflects the balance of production and loss processes of particulate matter. As such, POC is highest in surface waters where primary production is greatest and generally decreases with depth. In addition, particulate material can be moved from the surface into the deep ocean via gravitational settling or transport by physical and biological processes that also alter the composition and distribution of dissolved and suspended forms of organic carbon (Boyd et al., 2019). Accurate measurements of POC across time, space, platforms, and methodologies are important for understanding surface ocean ecology, creation and removal of POC throughout the water column, the sequestration of carbon into the deep ocean, and ultimately the impact of these processes on Earth's climate.

Methods for the collection and analysis of POC were described over 55 years ago (Menzel and Vaccaro, 1964) following shortly after or in tandem with those for measuring total and dissolved organic carbon (DOC) in seawater (Wilson, 1961; Menzel and Vaccaro, 1964). Menzel and Vaccaro (1964) described a method in which 1–4 L of seawater are filtered through a pre-combusted glass fiber filter with subsequent chemical analyses of the collected material. This approach is still common practice for "small volume" sample collection and analyses of POC concentrations from marine waters. Iterations and methodological considerations have evolved over time to include additional chemical analyses such as particulate nitrogen (PN) and particulate inorganic carbon (PIC), large volume sampling with in situ pumps (hundreds to thousands of liters) in order to sample rare large particles (Bishop and Edmond, 1976), multiple volume regression techniques for determining appropriate blank corrections (Moran et al., 1999), and procedural changes to eliminate artifacts due to collection techniques.

Comparisons between small volume bottle and large volume pump filtration generally show higher POC concentrations from bottles than pumps and in one instance differences up to multiple orders of magnitude were observed (Gardner et al., 2003). The discrepancies are typically attributed to differences in filter types, blank correction, filter holder types, and pressure differentials (Moran et al., 1999; Gardner et al., 2003; Liu et al., 2005; Liu et al., 2009). The retention properties of filters used for particle collection show some disparities within the literature. Whatman glass fiber, type F (GF/F) filters, with a nominal pore size of 0.7 μm or approximately 0.3 μm after combustion (Nayar and Chou, 2003), are commonly used for collecting POC using the small volume filtration technique (Moran et al., 1999). Some investigations revealed that certain cell or particle types pass through the GF/F filters while others showed no loss of particles or cells (Dickson and Wheeler, 1993; Chavez et al., 1995; Nayar and Chou, 2003). Large volume pump collections frequently use quartz fiber filters (Whatman QM-A) for analysis of carbon, major biological and lithogenic elements, and radionuclides because of lower blanks for many elements (Bishop et al., 1985) and radionuclides (Maiti et al., 2012) than GF/F filters. In large volume pumps QM-A filters are usually paired with larger pore size Nitex pre-screens for serial collection of multiple size fractions. QM-A filters have a manufacturer-stated nominal pore size of 2.2 μm prior to combustion but have been found to collect a particle population >1 μm when combusted and deployed in a paired configuration in large volume pump collections (Bishop et al., 2012).

Another confounding factor is the correct determination of non-target DOC, or what is referred to as an "adsorption blank." Multiple approaches have been devised to account for blanks, generally thought to be DOC adsorbing to filter material (Moran et al., 1999; Cetinić et al., 2012; Graff et al., 2015; Novak et al., 2018). While not explicit for DOC, the Menzel and Vaccaro (1964) process for measuring POC included a blank consisting of a pre-combusted filter briefly soaked in sample water. A similar method is currently used in large volume in situ filtration where blank filters are exposed to seawater for the same length of time and depth as the sample filters (Lam et al., 2015). In other approaches the carbon associated with a filter that has not been exposed to seawater, and only reflects the carbon intrinsic to the filter alone, is subtracted from the sample filter value (Knap et al., 1996). Many studies using the small volume filtration technique do not account or correct for blanks of filters exposed to seawater, yet blank values are commonly reported to be on the order of 10–20 μg C per 25 mm GF/F filter (Cetinić et al., 2012; Graff et al., 2015; Novak et al., 2018), which can be a significant portion of a POC filter for waters with a low particulate load. Aside from technical discrepancies, issues related to sample (mis)handling, lab and ship-borne contamination, and other commonly unrecognized or unmeasured artifacts can impact both accuracy and precision of POC data. For example, the contribution of live zooplankton to either pump or bottle samples has been considered as a reason for differences between methods (Liu et al., 2005) and could be considered a blank correction, but quantifying and subtracting this input from the total is difficult. A more thorough review and comparison of POC collection and measurement techniques can be found in

Chaves et al. (2021) and previous method comparison papers (Gardner et al., 2003; Liu et al., 2009).

The 2018 NASA EXport Processes in the Ocean from RemoTe Sensing (EXPORTS) field campaign provided an opportunity to compare POC results collected using multiple methodologies and platforms (Siegel et al., 2021). During the first field component for EXPORTS in the North Pacific Ocean near Ocean Station Papa, measurements of POC from inline flow-through seawater systems, CTD Niskin bottles, in situ pumps, and Marine Snow Catchers (MSCs) produced incongruent results. An analysis was undertaken to evaluate these disparities using a suite of synchronous or near-synchronous analytical and optical measurements and knowledge of technical details for each method. Particle size distributions (PSDs), phytoplankton pigments, and other supporting data were explored in the context of POC measurements, as well as specific sample handling, filters, and methodologies used to collect particles for carbon content analysis. Results include relationships of POC with inherent optical properties and a recommended approach for reconciling methodological differences between POC measured using bottles, in situ pumps, and MSCs.

## 2. Materials and methods

Samples for POC, PN, and related environmental parameters were collected from August 14 to September 9, 2018, in the North Pacific Ocean near Ocean Station P (approximately 50°N, 145°W) using multiple ships and platforms and including Niskin bottle rosettes, customized inline flow-through seawater systems, in situ pumps and MSCs. A detailed description of EXPORTS and its first field experiment in the North Pacific can be found in Siegel et al. (2021). Briefly, two ships were used to complete this field campaign. The R/V *Roger Revelle* (hereafter referred to as the "Process Ship") worked in a Lagrangian framework while the R/V *Sally Ride* (the "Survey Ship") measured the environmental conditions in a larger region centered about the Process Ship and a Lagrangian float. Niskin bottle and inline sampling occurred on both ships while MSCs were deployed from the Process Ship and in situ pumps were deployed from the Survey Ship. A map of the stations sampled during the expedition can be found in **Figure 1**. Particle sampling protocols for elemental analysis, phytoplankton flow cytometry, pigment analysis, and optical measurements are presented below. All data presented here and from the greater EXPORTS field

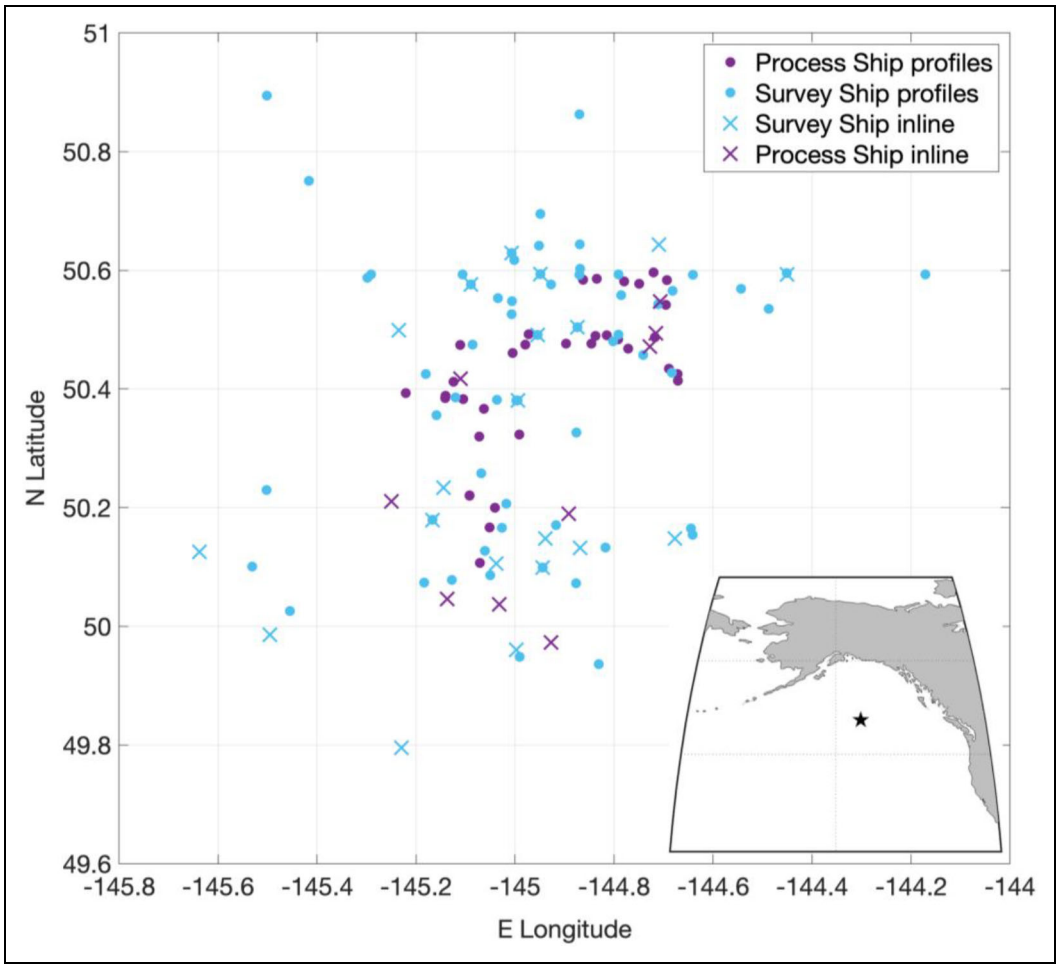


**Figure 1. Survey and Process Ship station map of the 2018 EXPORTS North Pacific field campaign.** Inset map shows the location of the sample region in the North Pacific Ocean denoted by a star. Survey and Process Ship profile and inline samples are identified by color and shape of symbols in the inset box.

experiment are found in the NASA SeaBASS data repository at https://seabass.gsfc.nasa.gov/experiment/EXPORTSNP.

### *2.1. Particulate organic carbon and nitrogen*

#### 2.1.1. Niskin bottle and inline sampling

Whole seawater for POC and PN samples was collected from 10 L Niskin bottles and inline flow-through seawater systems on the Process and Survey Ships (**Table 1**). Discrete depths were sampled using Niskin bottles mounted on a CTD rosette, with bottles closed on up-casts at predetermined depths. Survey Ship depths ranged from the surface down to 1000 m while the Process Ship focused on the upper approximate 100 m of the water column. Niskin bottles were outfitted with standard sampling spigots and were not inverted prior to sampling on deck. The seawater flow-through systems consisted of identical diaphragm pumps located at seawater intake ports at a depth of approximately 4 m. Science-supplied tubing, with the exception of a ship-supplied length of tubing on the Survey Ship, ran from the diaphragm pumps to the laboratories; the intake ports or sea chests were cleaned using bleach just prior to sailing. The diaphragm pump flow-through systems are designed to minimize disturbance of particles following specifications and recommendations in Boss et al. (2019a). The Survey Ship sampling scheme also utilized a second flow-through system with an intake located at a similar depth that consisted of the ship's stainless-steel impeller pump system and plastic plumbing.

Sampling on the Survey Ship followed three protocols. In the first, single whole seawater samples from each depth of CTD casts, hereafter referred to as "non-optics" casts, were collected directly from Niskin bottles into 2 L Nalgene bottles (exact volumes of bottles and volumes filtered were recorded and used in calculations in all protocols) within 15 minutes of CTD recovery and filtered immediately by inverting sample bottles with autosiphon caps into filter funnels. In the second, Niskin bottles from casts associated with early morning and approximate local noon profiles targeting optical and biological variables, hereafter referred to as "optics" casts, were drained down to the spigot into large volume carboys with half-inch tubing after waiting approximately 45 minutes for sampling of other variables and kept cold and dark until subsampling. In the third, whole seawater was collected directly into 2 L Nalgene bottles from the inline flow-through systems. Carboys from optics cast profiles were subsampled after approximately 2 hours, because of other sampling requirements, and immediately following sample homogenization by swirling three times in one direction, three times in the reverse direction, and three times in the first direction. Carboys were inverted to ensure full re-suspension before sampling. Subsamples were then collected into Nalgene bottles and decanted into the filtration funnels.

Process Ship sampling protocols were similar to those on the Survey Ship with some unique differences. All samples were collected directly from Niskins, after approximately 45 minutes after CTD recovery, or from the inline system into 2 L Nalgene bottles, with no large volume collections or subsampling from carboys as was performed for the optics casts on the Survey Ship. For all depths, single approximate 2 L volumes were filtered. For sample filtrations, Nalgene bottles were inverted into holders just above collection funnels. Sample bottle lids were outfitted with an autosiphon apparatus, similar to non-optics cast and inline sampling on the Survey Ship, that allowed for consistent replenishment of seawater into the funnel throughout the filtration process. All samples were filtered to completion and specific volumes recorded. Filtration times were relatively short, 30 minutes or less, given the generally low particle loads in water column, but exact times were not recorded. For a subset of samples ($n = 28$), a multiple volume regression approach was used to determine POC blanks (Moran et al., 1999). Here, samples of 0.5 L and 1 L were also collected alongside the 2 L sample. The 3-volume POC regression approach uses the intercept as an estimate of the blank correction, mainly due to DOC adsorption, needed to account for non-target carbon on a filter. A second blank was also collected by filtering the 1 L sample into a clean glass flask and then re-filtering the filtrate ($n = 26$). The average 1 L and intercept blanks were 1.05 μmol C and 1.25 μmol C and 0.15 μmol N and 0.16 μmol N, respectively. The average intercept blank from the Process Ship was applied to all samples collected from Niskin and inline systems irrespective of ship.

For all samples for POC, PN, and blanks collected as described above, whole seawater was filtered through pre-combusted 25 mm Whatman® GF/F discs (450°C, 4 hours) under low pressure (<5 cm Hg), wrapped in pre-combusted foil packets, and stored directly in liquid nitrogen or at −80°C until sample preparation and analysis. Pre-combusted filters were stored in batches (one batch for each CTD cast or inline sample) in individual, sealed Ziploc® plastic sandwich bags or in bulk in glass jars that had also been combusted with the filters and foil packets.

#### 2.1.2. In situ pump system

Size-fractionated particles collected using in situ pumps on the Survey Ship were analyzed for total particulate carbon (PC), PN, and PIC according to the methods detailed in Buesseler et al. (2020) and Roca-Martí et al. (2021; **Table 1**). Briefly, six in situ McLane pumps equipped with 142 mm-diameter mini-Multiple Unit Large Volume in situ Filtration System (MULVFS) filter holders (Bishop et al., 2012; Lam et al., 2015) were deployed on a total of 12 casts at 50 m, 100 m, 150 m, 200 m, 330 m, and 500 m (±5 m). Pumps were programmed to pump for 4–5 hours at a starting flow rate of 8 L minute$^{-1}$. Flow rate decreased during pumping as filters loaded, reaching an average minimum flow rate of 5.4 L minute$^{-1}$ at 50 m and 7.2–7.7 L minute$^{-1}$ at the deeper depths. On each filter holder, an approximate volume of 700–1500 L of seawater was passed sequentially through 51 μm and 5 μm pore-size Nitex (Sefar) screens followed by a pre-combusted (500°C, >12 hours) Whatman QM-A filter (2.2 μm nominal pore size before combustion). The nominal pore size post-combustion of QM-As is not fully resolved. Although the nominal pore size is

**Table 1. NASA EXPORTS platforms and methodological approaches for direct determinations of particulate organic carbon and particulate nitrogen**

| Ship | Approach | Collection | Approx. Volume Filtered (L) | Filter Type and Treatment | Effective Pore Size (μm) | Blank | Sample Handling Notes |
|---|---|---|---|---|---|---|---|
| Survey | Inline | bottle | 2 | Pre-combusted 25 mm GF/F (450°C, 4 hours) | 0.3 | Intercept (from Process Ship) | Filtered directly from collection bottle |
| | Optics profiles | Niskin/carboy/ bottle | 2 | Pre-combusted 25 mm GF/F (450°C, 4 hours) | 0.3 | Intercept (from Process Ship) | Niskin drained to spigot into carboy, subsampled after homogenization |
| | Non-optics profiles | Niskin/bottle | 2 | Pre-combusted 25 mm GF/F (450°C, 4 hours) | 0.3 | Intercept (from Process Ship) | Collected from Niskin, filtered directly from collection bottle |
| | *In situ* pumps | pump | 30–340 | Pre-combusted 142 mm QMA (500°C, >12 hours), 5 μm and 51 μm Nitex | 1.0, 5.0, 51 | Soaked, in situ | 21 mm QM-A punches from larger filter, equivalent of 1/3 of Nitex screens |
| Process | Inline | bottle | 2 | Pre-combusted 25 mm GF/F (450°C, 4 hours) | 0.3 | Intercept | Filtered directly from collection bottle |
| | All profiles | Niskin/bottle | 2 | Pre-combusted 25 mm GF/F (450°C, 4 hours) | 0.3 | Intercept | Collected from Niskin, filtered directly from collection bottle |
| | Marine Snow Catcher | MSC/bottle | 0.1–1 | Pre-combusted 25 mm GF/F (450°C, 0.5 hours) | 0.3 | Intercept (from Process Ship) | Subsampled from about 100 L MSC water or MSC collection tray, then filtered from collection bottle |

stated as 2.2 μm by the manufacturer, operational tests with paired combusted QM-As suggest that the top QM-A collects a population of particles close to 1 μm (Bishop et al., 2012). We assume that our single QM-A had a nominal pore size of 1 μm but note that a single QM-A, as deployed here, might not behave the same as paired QM-A and could potentially have a higher nominal pore size.

In addition, at three stations, a filter holder equipped with the same filters (51 μm and 5 μm pore-size Nitex, combusted QM-A) was mounted on the deepest pump to obtain "dipped blank" filters (Lam et al., 2015). On the dipped blanks, a prefilter (0.8 μm Supor) was placed on top of the 51 μm Nitex screen to avoid the collection of particles while filters were exposed to seawater. Handling of the filter holders and filters prior to and after collection was conducted within a clean-air bench (ISO 5 HEPA filter), except rinsing of the screens (see below), to minimize airborne contamination. Immediately after recovering the in situ pumps, residual water from all filter holders was removed by vacuum, and filter holders were kept refrigerated at 4°C until processing. Dipped blanks were processed in the same manner as the samples (Supor prefilter was discarded).

Swimmers (non-detrital zooplankton) visible to the naked eye were picked from the 51 μm screens. Particles were gently rinsed off the screens with 1 μm filtered seawater and collected onto 25 mm diameter, 1.2 μm pore-size silver (Ag) membrane filters (Sterlitech). Previous studies have documented that the rinsing step is able to remove >80% of the particulate material from Nitex screens (Buesseler et al., 1998). Filter processing was completed on average after 3.5 hours following pump recovery. All filters were dried in a 60°C oven at sea and stored until analysis. In the lab, the QM-A filters were subsampled using circular Teflon punches (21 mm diameter) and Ag filters were split into thirds by weight. Two different subsamples from the same filters were used for PC (and PN) and PIC determination. The equivalent volume of PC, PN, and PIC subsamples was on average 30 L for the QM-A punches and 340 L for the 1/3 Ag filters.

The PC, PN, and PIC average of the dipped blanks was subtracted from each measurement before dividing by the filtered volume. Blanks were on average <2% of total PC (1/3 Ag filter: 0.17 ± 0.28 μmol C; QM-A punch: 0.15 ± 0.21 μmol C) and <4% of total PN (1/3 Ag filter: 0.09 ± 0.05 μmol N; QM-A punch: below detection limit; Roca-Martí et al., 2021). In contrast, PIC concentrations were low (<4% of PC), and the relative contribution of the PIC blank to PIC measurements was >40% (1/3 Ag filter: 0.47 ± 0.03 μmol C; QM-A punch: 0.23 ± 0.01 μmol C). Triplicate QM-A punches from two samples (50 and 500 m) were also measured, obtaining a relative standard deviation (RSD) of 1%–5% for PC, 6%–8% for PN and 4%–5% for PIC. Pump data have an associated uncertainty from the blank correction (standard deviation) and the weighing error of the analytical balance used for splitting the filters. POC was obtained from the difference between blank-corrected PC and PIC results. Total pump POC (>1 μm) was obtained by adding POC concentrations from the three size fractions.

In addition to the sampling described above, three additional pump samples were collected through sequential 51 μm Nitex, 6 μm Nitex, paired QM-A, and paired GF75 filters (Sterlitech, 0.3 μm nominal pore size glass fiber) at depths of 20 m and 85 m, thus additionally sampling the 0.3–1.0 μm nominal size class. Filters were folded in pre-combusted aluminum foil and frozen at −80°C within 2 hours of collection, and later split by weight while frozen, freeze-dried, and subsampled by weight for bulk and amino acid analysis in the Close Lab at the University of Miami. Only the top filter of each set of paired filters was analyzed. Final concentrations were determined by dividing by the seawater volume analyzed in each subsample. A blank carbon contribution was determined from filters deployed identically to samples but with no volume filtered (failed pumps); no nitrogen was detectable in blank filters. The carbon blank was then subtracted, proportional to the surface area of filter analyzed for each sample. However, only PN concentrations are reported due to remaining uncertainties in carbon blank corrections. Amino acid quantification was conducted as described by Wojtal et al. (2023) and also included two samples collected at 320 m.

#### 2.1.3. Marine Snow Catchers

At 11 stations, the MSCs were deployed from the Process Ship to collect samples of suspended and sinking POC and PN from 3 depths between 20 m and 500 m (**Table 1**). The MSC (Lampitt et al., 1993) is a large water sampler (volume, 89.8 L; height, 1.5 m) with a removable base (approximately 8 L) that enables the separate collection of sinking particles (Riley et al., 2012; Giering et al., 2016). A full description of the MSC methodology has been published by Riley at al. (2012) and Giering et al. (2016). To collect fast-sinking particles, we modified the original protocol by placing a tray (height, 4.4 cm; area, 0.028 $m^2$; volume, approximately 1 L) at the bottom of the base of the MSC prior to each deployment (Romanelli et al., 2023). Briefly, within 1–2 minutes of retrieval, approximately 1 L was sampled from the central tap of the MSC to provide the total concentration of POC and PN present in the water column (T0 sample). After exactly 2 hours of settling time, 5 L of sample were collected from the central tap representing suspended particles. The top section of the MSC was drained slowly and detached from the base. Then, the water in the base overlying the tray was sampled; this water contains slow-sinking particles plus the existing suspended particles (approximately 5 L). Lastly, the water inside the tray, which contains fast-sinking particles plus the existing suspended and slow-sinking particles, was sampled (Romanelli et al., 2023). Samples were collected in closed narrow-mouthed low density polyethylene bottles. Approximately 1 L samples (or 0.1 L for the tray) were filtered each onto two replicate pre-combusted (450°C, 30 minutes) GF/F filters (25 mm, Whatman). Sample bottles were inverted onto the funnels and allowed to drain during filtration. Once empty, the bottles were removed, the filter funnels were rinsed with 0.2 μm filtered seawater, and filters transferred into Petri dishes. The filters were

dried at sea at 60°C and stored at room temperature in a desiccator until analysis (see CHN analysis below).

All POC values were above the detection limit (see *Elemental analysis*), while 23 of 214 PN values had to be omitted. Measured POC and PN values were corrected using the average intercept blank (see Niskin and Inline Sampling above). Slow-sinking POC and PN were calculated by subtracting the suspended POC and PN concentrations from concentrations measured in the base samples. Fast-sinking POC contributions were determined by subtracting the concentrations measured in the base (i.e., suspended and slow-sinking particles) from POC and PN concentrations measured in the tray samples. The differences were scaled for the volume ratios (Romanelli et al., 2023). We refer to the concentration of sinking particles as the sum of the concentration of slow- and fast-sinking particles. The standard sinking velocity of slow-sinking particles for the MSC is determined geometrically by dividing the sinking distance (height of the MSC) by the settling time (2 hours) and is 18 m $day^{-1}$ (Giering et al., 2016). Fast-sinking particles, which reached the MSC tray within the 2-hour settling time, sank at an average sinking velocity >18 m $day^{-1}$. Hence an average sinking velocity of 18 m $day^{-1}$ represents a conservative average of the sinking velocity of sinking particles because fast-sinking particles could have reached the tray of the MSC much sooner than 2 hours (Giering et al., 2016).

#### 2.1.4. Elemental analysis

All POC and PN samples from Niskin, inline, and MSC samples were analyzed at the University of California, Santa Barbara Marine Science Institute Analytical Lab (https://msi.ucsb.edu/facilities-services/analytical-lab/about). Filters were saturated briefly with hydrochloric acid (<5 minutes, 10% v/v) applied by a dropper in order to remove inorganic carbon and immediately moved to a vented 60°C drying oven. Dry filters were analyzed on an Exeter Analytics CEC 440HA. POC and PN concentrations were determined by subtracting the 3-volume intercept blank, as described above for Process Ship sampling, from the reported masses and dividing by the volume filtered specific to each sample. POC and PN detection limits ranged between 0.8 μg and 16 μg and between 0.2 μg and 3.9 μg, respectively.

In situ pump samples were analyzed at the Woods Hole Oceanographic Institution (Roca-Martí et al., 2021). Total particulate carbon and PN were analyzed at the Nutrient Analytical Facility using a high-temperature combustion technique. Dried particulate samples were prepared inside an ultra-clean tin disk and combusted at high temperature. Total particulate carbon was converted into carbon dioxide and nitrogen into nitrogen gas. These elements were separated by gas chromatography and measured by thermal conductivity on an Elemental Microanalysis Flash EA 1112 (Ehrhardt and Koeve, 1999). PIC was determined by closed-system digestion with phosphoric acid by coulometry (Honjo et al., 1995), and POC was determined as the difference between total particulate carbon and PIC. Additional pump samples from 20 m and 85 m were analyzed for PN on a Thermo Flash Elemental Analyzer interfaced to a Conflo IV and MAT 253 isotope ratio mass spectrometer; $CO_2$ and $N_2$ peak areas acquired during natural abundance stable isotope analysis were also used to quantify carbon and nitrogen in comparison to standards.

### 2.2. Phytoplankton pigments

Samples were collected for HPLC phytoplankton pigment analysis using the aforementioned collection methods for POC and PN from Niskin bottles and inline systems, as well as QM-A filter subsamples from the McLane pumps. For Niskins and inline systems, whole seawater was collected directly into 2 L Nalgene bottles and filtered immediately via low pressure (<5 cm Hg) vacuum filtration onto pre-combusted (450°C, 4 hours) 25 mm Whatman® GF/F filters. Subsamples from large carboys collected during Survey Ship optics casts were drawn into 2 L Nalgene bottles after sample homogenization. Each sample was filtered immediately via low pressure vacuum onto a pre-combusted 25 mm diameter Whatman® GF/F filter. Subsamples from the pump QM-A filters consisted of one circular 25.3 mm diameter Teflon punch collected after pump recovery. Nitex screens were not subsampled for pigments. Thus, pump pigment data only represent the 1–5 μm fraction.

All HPLC samples, regardless of platform, were frozen in liquid nitrogen or at −80°C immediately following filtration. Samples remained frozen until processing at the NASA Goddard Space Flight Center, following strict quality assurance and quality control protocols (Van Heukelem and Hooker, 2011; Hooker et al., 2012). All pigment values measured below the HPLC method detection limits for each pigment were set equal to zero in this dataset. The HPLC pigments used in this analysis (and their abbreviations) are total chlorophyll-*a* (Tchla), fucoxanthin (Fuco), peridinin (Perid), and zeaxanthin (Zea). The three accessory pigments were chosen based upon their established relationships with specific phytoplankton groups and to some extent size classes: diatoms (Fuco), dinoflagellates (Perid), and cyanobacteria (Zea; e.g., Jeffrey et al., 2011; Kramer et al., 2020).

### 2.3. Particle size distribution

A Laser In-Situ Scattering and Transmissometry—Volume Scattering Function (LISST-VSF, Sequoia Scientific, Inc.; Bellevue, WA) was used to measure the volume scattering function from 0.08° to 155° at 517 nm. Approximately 1.8 L of whole seawater collected from Niskin bottles at multiple depths during optics casts on the Survey Ship were pumped peristaltically into the sampling enclosure. Then, the residual bubbles (usually none) were removed by a debubbler to the sampling enclosure of the LISST-VSF. The LISST-VSF was turned on for 30 minutes for the laser to stabilize before measurement. For each water sample, 30 repeated measurements of angular scattering from 0.08° to 155° were taken, and the median values of the measurements at each scattering angle were used to form the VSF for each sample following the procedure described in Hu et al. (2019b).

The size distributions and the refractive index of the particles were estimated from the VSFs using the VSF-inversion method described in detail in Zhang et al. (2011) and refined in Twardowski et al. (2012) and Zhang et al. (2012). The PSDs estimated from this VSF-inversion approach have been found to agree (within 10%) with the particle distribution obtained using the laser diffraction approach (Zhang et al., 2012). In this study, results from the particle distributions obtained using a Coulter Counter, an Imaging Flow CytoBot, laser diffraction approach, and a Brownian motion approach, were compared and agreed within 50% (±1 SD) after correcting the bias due to the differences in defining sizes by different approaches (Zhang et al., 2023). The volume distribution of the particles was estimated by accounting for the fractal nature of oceanic particles (Khelifa and Hill, 2006). Because the refractive index is closely related to the density of particles (Aas, 1996), the particle density was estimated using the empirical relationship established between the refractive index and the density for oceanic particles (Morel and Ahn, 1990; Babin et al., 2003). The volume and density distribution data thus obtained were then used to calculate the mass-size distribution of particles. The methodological details of estimating the mass distribution from the VSF-inverted PSD are provided in Zhang et al. (2014). For this study, the mass-size distribution for organic matter was the focus and was defined as those particles with a refractive index of less than 1.10 relative to water (Aas, 1996).

### 2.4. Phytoplankton flow cytometry

Flow cytometry (FCM) determinations of phytoplankton groups were conducted on live samples collected from Niskin bottles and the inline system aboard the Process Ship. Detailed descriptions of the methods used during EXPORTS can be found in McNair et al. (2021) and Graff and Behrenfeld (2018). Briefly, whole seawater was collected into 5 mL polycarbonate tubes and analyzed within 30 minutes of collection on a Becton Dickinson Influx Cell Sorter (ICS). The ICS is equipped with a 488 nm excitation laser and detectors for forward scatter (FSC), side scatter (SSC), and fluorescence at 530 nm and 690 nm, properties used here to discriminate *Synechococcus*, picoeukaryote, and nanoeukaryote groups. Time length of sample analysis and sample flow rates determined at sea were used to calculate in situ concentrations.

### 2.5. Particulate beam attenuation and backscattering

Optical beam attenuation ($c_p$) and particulate backscattering ($b_{bp}$) were measured from the CTD rosette on both the Survey and the Process ships, detailed methods can be found in EXPORTS NP Science Team (2021). All sensors on the rosette were placed at the bottom of the rosette with clear access to undisturbed water on down casts and maintained throughout the cruise (e.g., cleaning, calibrations) following community-derived recommendations in the IOCCG Protocol Series (Boss et al., 2019b). Particulate backscattering at 700 nm was calculated from Seabird ECO sensors on board each CTD rosette as:

$$b_{bp} = 2\pi(\beta - \beta_{sw})\chi_p \quad (1)$$

where $\beta$ is the measured volume scattering function, after subtracting the dark value from taped casts, at 700 nm and 142°; $\beta_{sw}$ is the pure seawater volume scattering function (Zhang and Hu, 2009); and $\chi_p = 1.14$ is a conversion factor determined specifically for the EXPORTS North Pacific deployment (Zhang et al., 2021). Because this study focuses on the upper 500 m of the water column, the effect of pressure on seawater scattering (Hu et al., 2019a) was not accounted for; it should be considered for depths >1000 m. Optical measurements from the Process Ship had instrument fluctuations over the first part of the cruise but stabilized after 16 days. After the Process Ship measurements stabilized, Erickson et al. (2022) determined that a relatively minor change in scaling factor (×0.95) and offset ($-1.0 \times 10^{-4}$ m$^{-1}$) for the Survey Ship was required to best align the two platforms. In-depth details regarding the optical data collection and intercalibration efforts can be found in Erickson et al. (2022).

Beam attenuation was measured on each ship using Seabird C-star instruments at 650 nm. The instruments were corrected for a time-dependent calibration drift, and profiles containing anomalously high values at depth were discarded. An offset of $-0.04$ m$^{-1}$ was applied to the Process Ship to align its mean $c_p$ at 500 m with that of the Survey Ship. Profiles that did not descend to at least 500 m, or profiles with $c_p$ values at 500 m significantly different (±0.005 m$^{-1}$) than the median value for each ship, were discarded. After these steps, remaining uncertainty for each platform is estimated to be 0.001 m$^{-1}$ as reported in the supporting documents for the NASA EXPORTS optical datasets (https://seabass.gsfc.nasa.gov/experiment/EXPORTS).

## 3. Results

Methodological constraints culminated in variable sample volumes, filter types, pore sizes, and sample handling procedures; each difference has the potential to impart variability in particle concentrations. **Table 1** summarizes each method described herein and the similarities and differences between them. Methodologically, Niskin and inline sampling was similar for both ship-based small volume sampling, with the exception of large volume collection into carboys, homogenization, and subsampling on the Survey Ship during casts associated with co-located optical measurements. In situ pumps differed from Niskin and inline sampling by both the volume of samples (on the order of 10s–100s L versus 2 L), filter type and pore size (QM-A versus GF/F) and that the pumps operate at an initial 60 cm Hg versus 5 cm Hg for Niskin-collected samples. Sampling of the MSC was similar to Niskin sampling with respect to volume and filter type but provided an opportunity to separate particles with respect to their sinking velocity and to evaluate the contribution of sinking particles. Knowledge

about these differences is applied in order to understand the methodologically driven offsets in the datasets they provided.

### *3.1. POC, PN, and POC:PN*

All methods showed similar depth trends with high POC and PN at the surface and decreasing concentrations with increasing depth in the water column (**Figure 2A** and **B**). **Table 2** provides summary data (means and standard deviations) for discrete depth horizons across approaches and platforms. Process Ship POC and PN from Niskin bottles averaged 4.1 and 0.67 µmol $L^{-1}$ in the top 10 m while the Survey Ship Niskin samples were higher by approximately 2 and 0.2 µmol $L^{-1}$ for POC and PN, respectively (**Table 2**). Samples from the two inline systems were also offset with slightly higher values measured on the Survey Ship (pink symbols in **Figure 2A** and **B**). At 95–110 m, concentrations had decreased to 1.4 µmol $L^{-1}$ POC and 0.21 µmol $L^{-1}$ PN for the Process Ship, with Survey Ship values still higher, albeit a less absolute difference than samples at the surface. In situ pump POC and PN concentrations from 50 m were 1.5 and 0.26 µmol $L^{-1}$ (n = 11) for POC and PN, respectively, decreasing to 0.18 and 0.026 µmol $L^{-1}$ (n = 12), respectively, by 500 m when combining all size fractions (gold circles in **Figure 2A** and **B**; **Table 2**). While the Process Ship rarely sampled below 110 m, POC from the Survey Ship at 500 m averaged 2.1 µmol $L^{-1}$ (n = 22, with one outlier at 14.6 µmol $L^{-1}$ removed). Similar depth trends were also found in the MSC samples. Average POC was 6.1 µmol $L^{-1}$ at 20–25 m (n = 2), 4.4 at 50–65 m (n = 10), 2.3 (n = 8) at 95 m and 1.0 (n = 7) at 300–500 m. The strongest decline in POC and PN occurred below 50 m for all platforms and methods.

In contrast to the other methods, the MSC provides the unique ability to evaluate the contribution of slow- and fast-sinking particles to POC and PN. Concentrations of total sinking (fast- plus slow-sinking) POC ranged from 0.03 to 2.9 µmol $L^{-1}$, with an overall average of 0.38 µmol $L^{-1}$ or an average for the upper 110 m of 0.42 µmol $L^{-1}$. For 23 of 27 deployments, the sinking POC contribution was low, varying between 0.1 and 0.4 µmol $L^{-1}$. Total sinking POC was negligible in one deployment but was >1 µmol $L^{-1}$ in three other samples collected at depths to 350 m, with two of these three "high" values collected from the same station. If only fast-sinking particles rather than total sinking particles are considered, on average 0.1 ± 0.1 µmol $L^{-1}$ (n = 26) POC sank, with two exceptions where an average of 1.3 ± 0.4 µmol $L^{-1}$ (n = 2) POC sank within 2 hours. Total sinking PN concentrations ranged between 0.01 and 0.28 µmol $L^{-1}$. As for POC, the sinking PN contribution was low in 23 of 26 deployments, varying between 0.01 and 0.09 µmol $L^{-1}$, whereas in three deployments, total sinking PN concentrations were well over 0.1 µmol $L^{-1}$ as deep as 350 m. These were the same deployments that showed high concentrations of sinking POC. If only fast-sinking particles

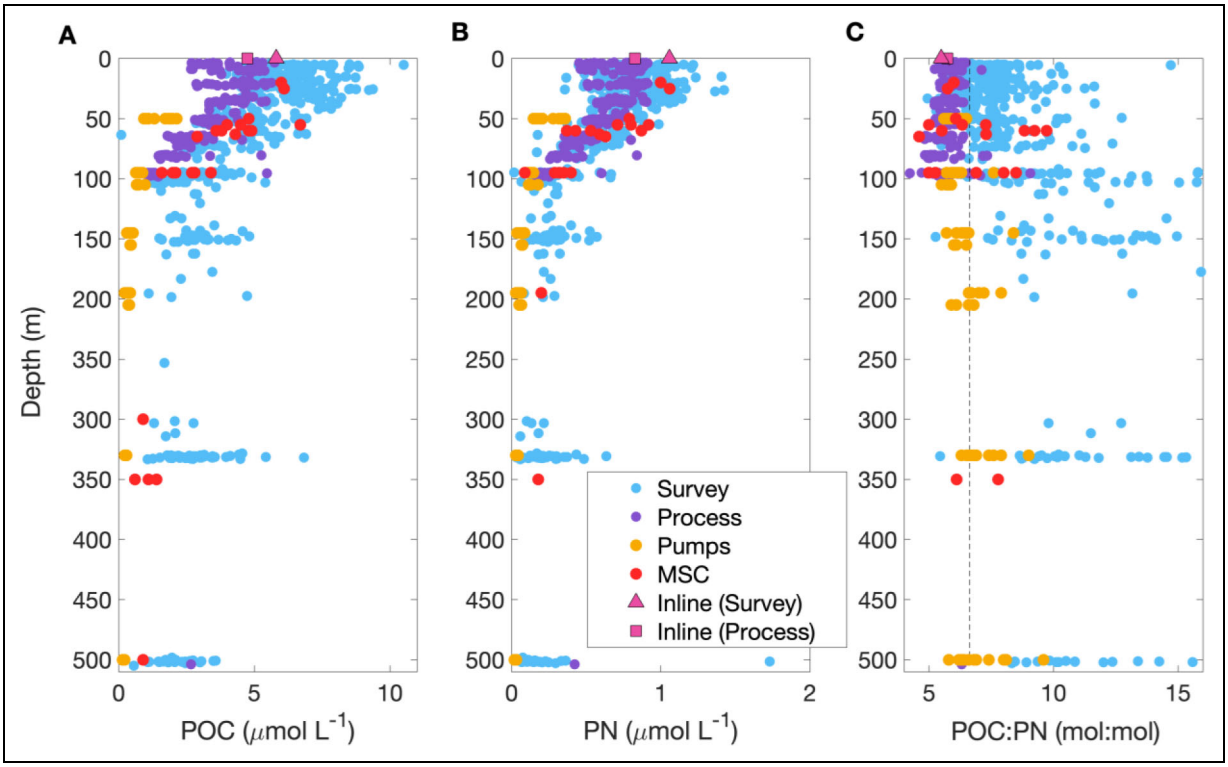


**Figure 2. Depth profiles of particulate organic carbon (POC), particulate nitrogen (PN) and their ratio (POC:PN).** Concentrations (µmol $L^{-1}$) of (A) POC and (B) PN and ratios of (C) POC:PN (mol:mol) from multiple sampling platforms, including the Survey (light blue) and Process (purple) ships, in situ pumps (gold), Marine Snow Catchers (MSCs, red), and custom inline systems on both ships (mean values, pink). Vertical dashed line in panel C is the C:N Redfield ratio of 6.6. No corrections beyond an initial blank correction have been applied to these data.

**Table 2. NASA EXPORTS North Pacific particulate organic carbon (POC) and particulate nitrogen (PN) concentrations (μmol $L^{-1}$) at discrete depth horizons**

| Depth Range (m) | Platform/Approach | POC (±SD) | PN (±SD) | n = (POC, PON) |
|---|---|---|---|---|
| 0–10 | Process CTD | 4.1 (0.9) | 0.67 (0.17) | 29, 29 |
| | Process inline | 4.8 (0.7) | 0.83 (0.11) | 13, 13 |
| | Survey CTD | 6.5 (1.6) | 0.87 (0.22) | 43, 43 |
| | Survey inline | 5.8 (2.1) | 1.06 (0.41) | 21, 21 |
| | Marine Snow Catcher* | 6.1 | 1.04 | 2, 2 |
| | In situ pump | None | None | 0, 0 |
| 45–55 | Process CTD | 3.5 (0.4) | 0.54 (0.03) | 25, 25 |
| | Survey CTD | 4.8 (1.0) | 0.65 (0.14) | 41, 41 |
| | Marine Snow Catcher | 4.4 (1.0) | 0.66 (0.18) | 4, 4 |
| | In situ pump | 1.5 (0.5) | 0.26 (0.08) | 11, 11 |
| 95–110 | Process CTD | 1.4 (1.1) | 0.21 (0.05) | 17, 17 |
| | Survey CTD | 2.9 (1.0) | 0.29 (0.13) | 42, 43 |
| | Marine Snow Catcher | 2.3 (0.6) | 0.29 (0.14) | 8, 7 |
| | In situ pump | 0.7 (0.1) | 0.12 (0.02) | 12, 12 |
| 490–510 | Process CTD | None | None | 0, 0 |
| | Survey CTD | 2.1 (0.8) | 0.17 (0.09) | 13, 22 |
| | Marine Snow Catcher* | 1.0 (0.04) | 0.13 (0.07) | 3, 2 |
| | In situ pump | 0.18 (0.02) | 0.026 (0.004) | 12, 12 |

*Shallowest surface samples for MSC were collected from 20 to 25 m; deepest range reported is for samples from 300 to 350 m.

are considered, on average 0.02 ± 0.02 μmol $L^{-1}$ (n = 24) PN sank to depth, with one exception where 0.15 ± 0.06 μmol $L^{-1}$ (n = 1) PN sank.

While the general trends with depth for POC and PN are preserved between platforms and methods, their differences are apparent in the absolute values (**Figure 2A** and **B**) and in the relative changes observed in the POC:PN ratios (**Figure 2C**). Much higher overall POC concentrations in the Survey Ship Niskin samples resulted in molar ratios higher than those found in the other approaches and are most noticeable at depths at or below 50 m, where POC:PN values frequently exceeded 10. While differences between inline samples from each ship were apparent in their absolute values, the stoichiometric ratios were not significantly different at 5.7 and 5.5 for the Process and Survey Ships, respectively. Stoichiometric ratios from in situ pumps and MSCs are in general agreement with those measured in the Process Ship Niskin samples and inline samples from both ships (**Figure 2C**). These results indicate that significant corrections are required for both POC and PN in order to properly compare multiple datasets.

### *3.2. Phytoplankton pigments*

Profiles of Tchla, Zea, Fuco, and Perid from all platforms and approaches exhibit generally similar depth trends, with subtle differences (**Figure 3A**–**D**) indicative of photoacclimation and changes in community composition with depth. Tchla and Fuco display broad subsurface maxima, while a sharp subsurface maximum in Zea from approximately 40–65 m presents a much more punctuated depth profile. The Perid profile reveals some indications of a subsurface maximum between 20 m and 40 m, but lacks the defined vertical trend seen in the other three pigments. Inline sample values are also included in **Figure 3** (pink symbols) for each ship. Inline samples from the Process and Survey Ships agree well with the shallowest Niskin samples collected from the same platform, as well as across platforms. Similar to the POC and PN dataset, in situ pumps resulted in lower pigment concentrations (**Figures 3** and **4**), although, unlike for POC and PN, the pump dataset represents only pigment concentrations in the smallest size fraction collected on QM-A filters (Nitex screens were not subsampled for pigments; Section 2.2). From all pigments analyzed, Zea, a pigment largely diagnostic for picophytoplankton, is the pigment that shows the largest difference between pumps and bottles, especially around 50 m. Zea was consistently much higher in bottles than in pumps at this depth with an average concentration of 0.013 ± 0.005 mg $m^{-3}$ (n = 65, combined ship data) compared to 0.0018 ± 0.0008 (n = 11) for pumps at 45–55 m, which was only 14% of Niskin Zea samples. Tchla, Fuco and Perid also show discrepancies between pumps and bottle samples but to a lesser extent than Zea. Mean total Niskin Tchla at 50 m was 0.25 ± 0.06 mg $m^{-3}$ (n = 65, combined ship data) versus 0.15 ± 0.04

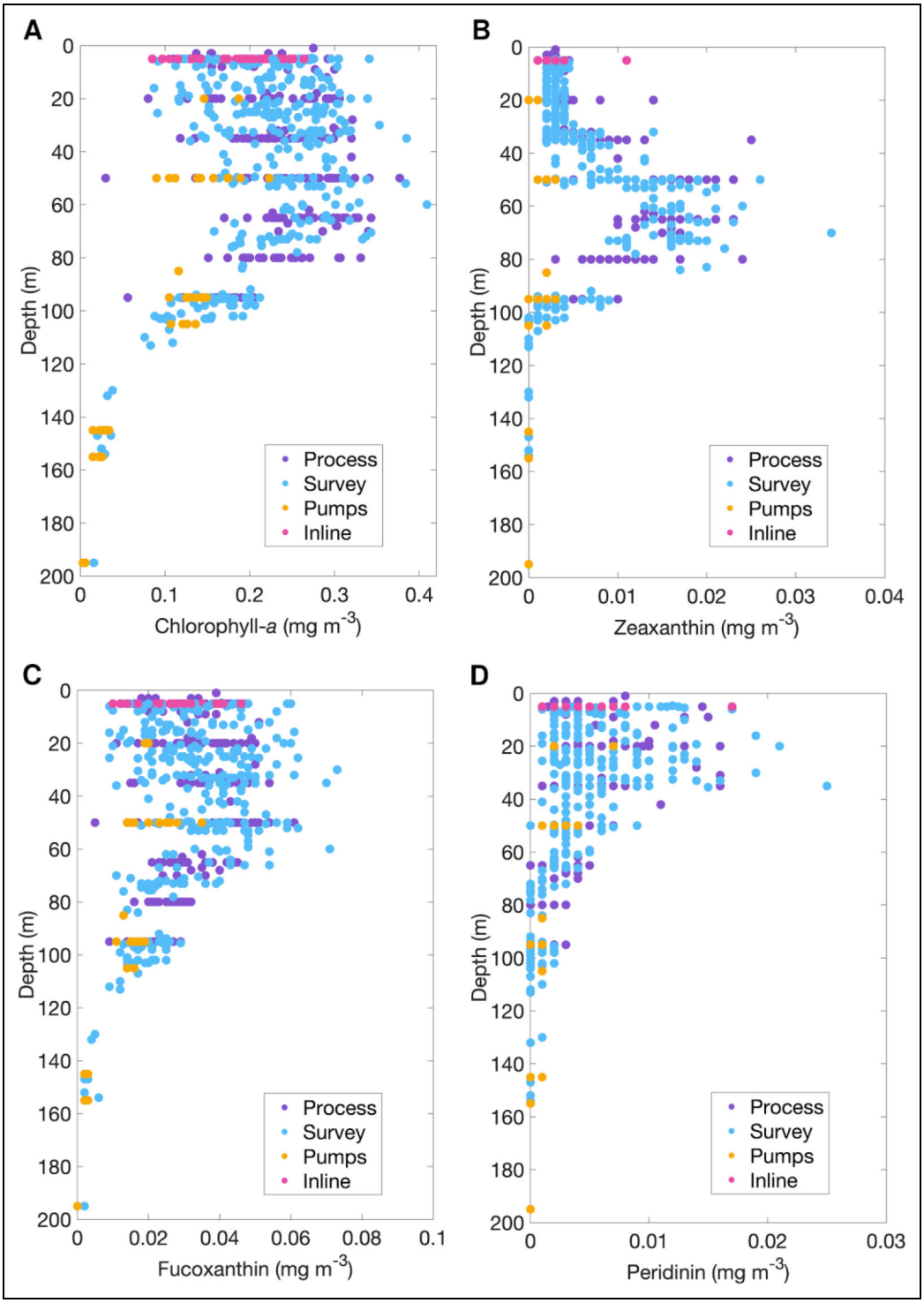


**Figure 3. Depth profiles of select phytoplankton pigments by high-performance liquid chromatography (HPLC).** Pigments were selected from HPLC analysis to help understand platform sampling differences: (A) total chlorophyll-*a*, (B) zeaxanthin, (C) fucoxanthin, and (D) peridinin. Samples were collected from Survey and Process ships (light blue and purple, respectively), in situ pumps (gold), and inline systems (pink). The pump pigment dataset represents only the smallest size fraction collected on QM-A filters (1–5 µm fraction).

mg $m^{-3}$ (n = 11), or 59% of Niskin Tchla, from pumps. Mean total Niskin Fuco at 50 m was 0.040 ± 0.011 mg $m^{-3}$ (n = 65) versus 0.022 + 0.007 mg $m^{-3}$ (n = 11) from pumps (55% of Niskin Fuco), and mean Niskin Perid at 50 m was 0.0037 ± 0.0019 mg $m^{-3}$ (n = 65) compared to 0.0020 ± 0.0009 mg $m^{-3}$ (n = 11) from pump samples (54% of Niskin Perid). The lower concentrations of Tchla, Fuco and Perid found from pumps relative to bottles can be attributed to a great extent to the fact that pump pigment samples excluded cells >5 µm (average fraction of Tchla on the >5 µm size class at 50 m was 28% ± 5%, n = 3; Meyer et al., 2022).

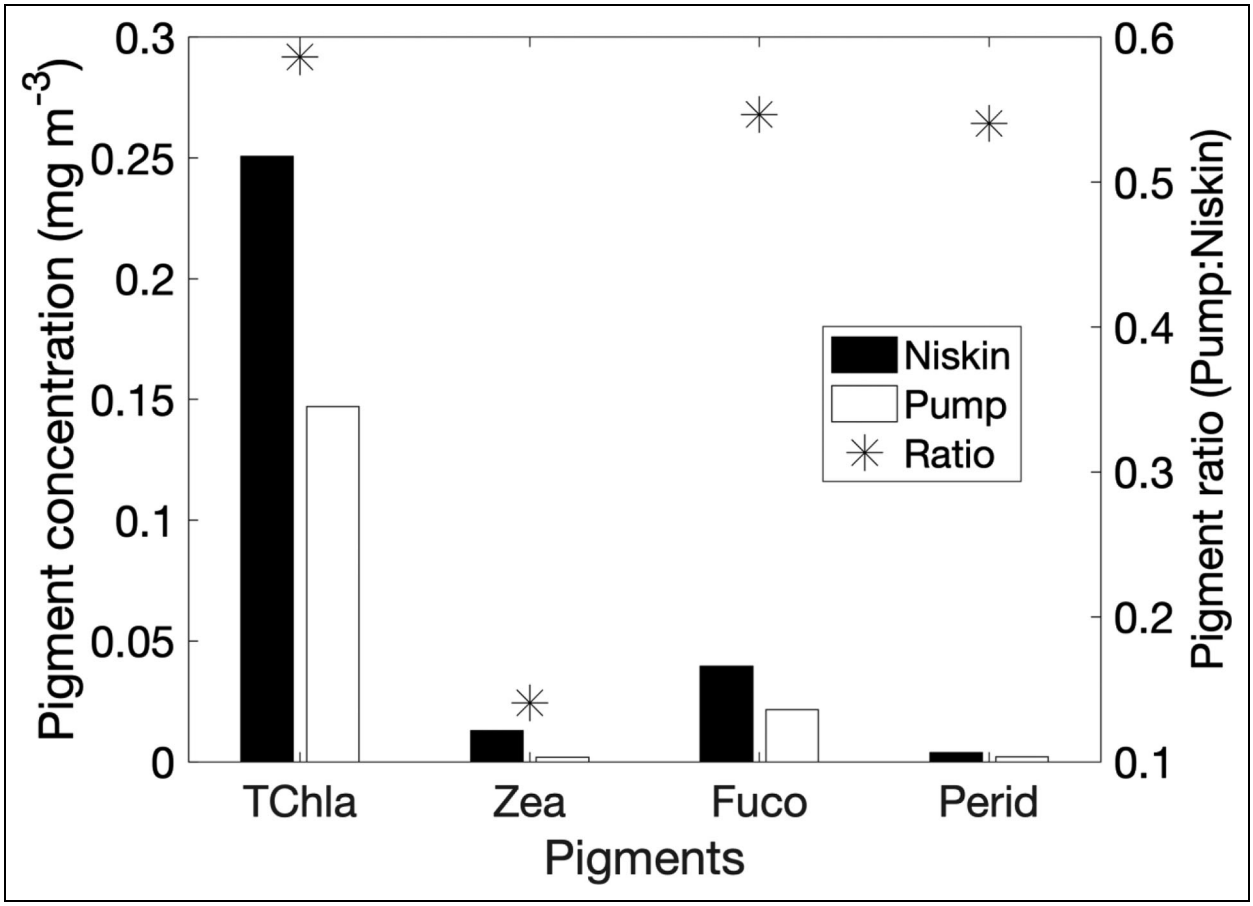


**Figure 4. Comparison of select pigments, collected from Niskin bottles and in situ pumps, and pump-to-Niskin ratios.** Selected high-performance liquid chromatography pigments, collected at 45–55 m depths from Niskin bottles and in situ pumps on the Survey Ship, are compared directly as mean concentrations of total chlorophyll-*a* (TChla), zeaxanthin (Zea), fucozanthin (Fuco), and peridinin (Perid), and as the ratio of pump-to-Niskin concentrations (asterisks). The pump pigment dataset represents only the smallest size fraction collected on QM-A filters (1–5 μm fraction).

### *3.3. Particle and phytoplankton size distributions*

Particle mass distributions from the VSF inversion method conducted on the Survey Ship suggest that particles from 0.2 μm to 1 μm were on average 35% (±9%) of particulate organic matter (POM) in samples collected from the surface down to 3000 m. **Figure 5A** shows the fraction of the total POM for this size class from samples collected in the upper 200 m. Phytoplankton groups, observed from flow cytometry on the Process Ship, displayed more distinct patterns with depth (**Figure 5B**), similar to HPLC pigments. The small prokaryote *Synechococcus* has a distinct subsurface maximum in abundance from 40 m to 65 m, similar to that found in the Zea profiles. Pico- and nano-eukaryote groups are relatively consistent in abundance from the surface down to 75 m, with minor increases from 50 m to 75 m. All groups decrease rapidly in abundance below 85 m. These optical data show general similarity with profiles from HPLC pigments, reinforcing the use of pigments to indicate phytoplankton taxa. These results also highlight the importance of relatively small phytoplankton, such as *Synechococcus*, in this region.

In situ pump PN and amino acid concentrations for a 0.3–1.0 μm size fraction are reported by Wojtal et al. (2023). Briefly, in two samples collected at 20 m, the 0.3–1.0 μm size fraction contained approximately 17% and 35% of PN, and in one sample collected at 85 m, this size fraction contained approximately 24% of PN. Particles ≥6 μm constituted approximately 3%–6% of PN, with the remainder of PN captured in the 1.0–6 μm size fraction. While POC is not reported by Wojtal et al. (2023), the C:N ratios were generally consistent across size classes such that POC is assumed to parallel these size distributions in PN. Determination of amino acid concentrations was less precise methodologically than bulk PN (Wojtal et al., 2023), but the size distributions were nonetheless similar, with approximately 15%–30% of particulate amino acids captured in the 0.3–1.0 μm size fraction at the 20 m and 85 m depths. Additionally, results from the 0.3–1.0 μm size fraction were reported for two samples collected at 320 m, where this size fraction constituted a smaller proportion of total particulate amino acids (<10%).

### *3.4. Optical profiles*

Cruise average (1 m binned) profiles of $c_p$ and $b_{bp}$ depict similar trends for each ship (**Figure 6**), with higher values found in the surface mixed layer (approximately 30 m;

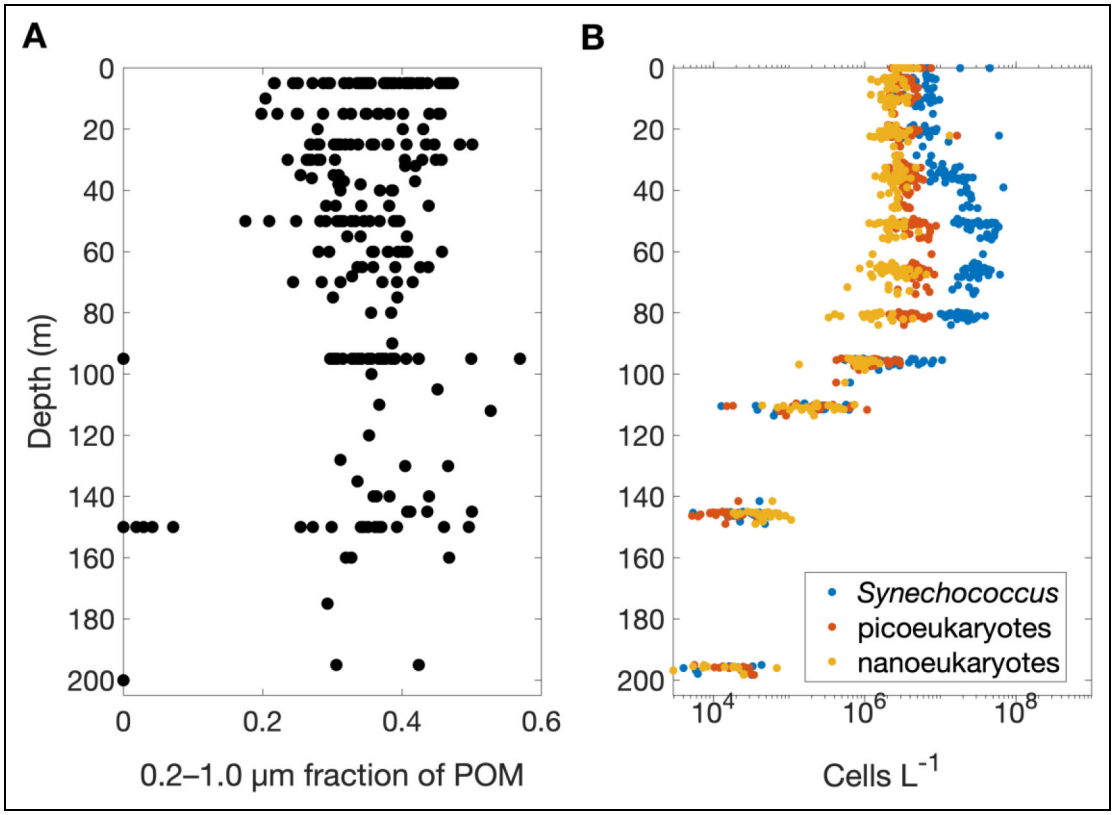


**Figure 5. Depth profiles of small particle contributions to particulate organic matter and of phytoplankton concentrations.** Vertical distributions of (A) the contribution to particulate organic matter (POM) from 0.2 to 1.0 µm sized particles and (B) phytoplankton concentrations are shown from surface to 200 m. The contributions of small (0.2–1.0 µm) particles to POM were determined from volume scattering function (VSF) inversion algorithms to determine particle sizes. *Synechococcus*, picoeukaryote and nanoeukaryote phytoplankton groups were determined by flow cytometry.

Siegel et al., 2021) and decreasing with increasing depth. Subsurface maxima can be seen, particularly in $b_{bp}$ profiles (**Figure 6B**), from approximately 50 m to 70 m. This optical feature corresponds with peaks observed for some pigments, particularly Zea (**Figure 3A** and **B**), and in phytoplankton cell concentrations (**Figure 5B**) at these depths. The Survey Ship sampled a larger region and number of water masses (Siegel et al., 2021), and the median $b_{bp}$ values near the surface, after aligning this instrument to the Process Ship using nearby casts (Erickson et al., 2022), are larger than those sampled by the Process Ship.

## 4. Discussion

Measurements of POC, PN, and POC:PN obtained using multiple methodologies can be difficult to compare. Even seemingly small differences, similar to those observed here (about 2 µmol), are important in waters where the total POC concentration is small and/or when values are integrated over greater depths or surface areas. Fortunately, strengths and weaknesses of each protocol and supporting datasets such as HPLC pigments, PSD, and phytoplankton community composition can provide insights for normalization across methodologies. **Table 1** served as an initial guide for identifying methodological differences that potentially led to divergent POC results and helped to identify datasets that could be utilized for reconciling methods. The scientific roadmap to understanding methodologically driven discrepancies in datasets in this study can be found in **Figure 7** and in the discussion that follows.

### *4.1. Measurement comparisons and reconciliation*

#### 4.1.1. Niskin samples from Survey and Process Ships (Step 1 in Figure 7)

Despite analysis at the same facility and application of the same regression-based blank to all samples collected from Niskin and inline systems, Survey Ship POC samples were significantly higher by about 2 µmol $L^{-1}$ than those measured on the Process Ship. PN samples were also higher, by a smaller amount (approximately 0.2 µmol $L^{-1}$; **Figure 2A** and **B**). While the higher POC:PN ratios observed in the Survey Ship samples were similar to Redfield, they increased to ratios in excess of 10 at depth (**Figure 2C**). A comparison of the two datasets restricted to the depths of sampling of the Process Ship (upper approximate 110 m) using a Kolmogorov-Smirnov test (Matlab, kstest2) indicated that the Survey and Process ship measurements differed significantly (POC, $p = 3.8 \times 10^{-6}$; PN, $p = 4.6 \times 10^{-5}$). Cumulative distribution plots of the POC and PN datasets can be found in Supplemental Figure S1.

A review of the methods highlighted that on the Survey Ship, two sample handling protocols were employed for

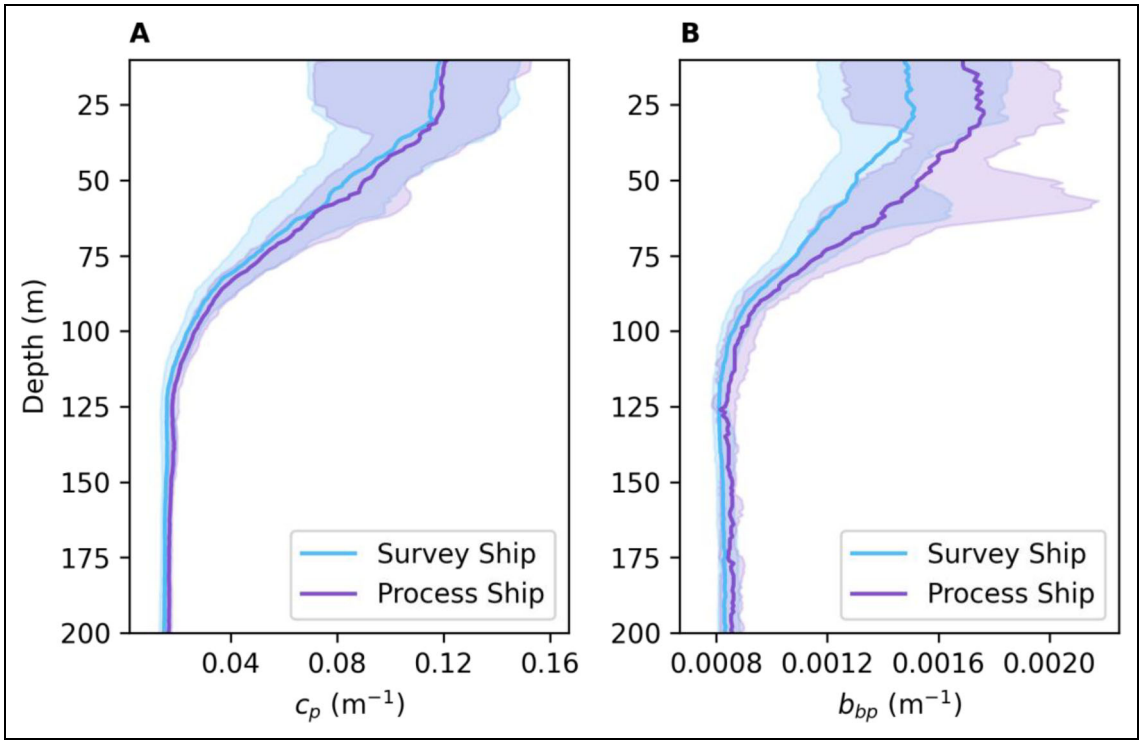


**Figure 6. Depth profiles of beam attenuation and particulate backscattering measured from two ships.** Cruise profiles of the median 1 m binned optical properties of (A) particulate beam attenuation ($c_p$) and (B) particulate backscattering ($b_{bp}$) were collected from the Process (purple) and Survey (blue) ship CTD rosettes. Shaded areas outline the 10–90th percentiles.

CTD Rosette casts. First, there were large volume collections into carboys that included homogenization and subsampling and were associated with co-located optics profiles, while a second protocol included sampling from the Niskin bottles into 2 L Nalgene bottles for direct filtering and was used during non-optics associated casts, the latter of which was identical to that on the Process Ship. This discrepancy provided the opportunity to evaluate how different sample collection techniques might drive dataset disparities, as well as to investigate possible systematic differences between ships. Separating the data by collection method on the Survey Ship (optics versus non-optics casts; **Figure 8A–C**) suggested that POC data from optics casts were higher than the non-optics casts, by an average of approximately 1 µmol $L^{-1}$ compared to the 2 µmol $L^{-1}$ difference between ships, and indicate two separate issues: one based on sample handling differences on the Survey Ship and one due to differences between ships when sampling from the rosette.

Both ships also collected underway samples from the inline seawater systems, representing a third sample collection method with respect to collection and filtering techniques. The inline samples of the Survey Ship and Process Ship had a similar offset (around 1 µmol $L^{-1}$ POC) to that of Niskin sampling and were from significantly different distributions (Matlab, kstest2, $p = 0.034$) (pink symbols in **Figure 8A**). PN datasets were more closely aligned across all platforms and methods, with some noticeable offsets in the optics casts collection from the Survey Ship (**Figure 8B**). The greater differences in POC than PN, resulting in higher POC:PN, suggested that additional corrections, beyond the blanks derived from the Process Ship that had already been applied to all data, were required for the Survey Ship due to possible ship-based contamination and/or differences in sample collection and handling, with the latter varying significantly between optics and non-optics associated casts on the Survey Ship (**Table 1**).

To further reconcile the Process Ship and Survey Ship bottle POC and PN results, Niskin bottle data were isolated by cast type and then spatially filtered to reduce differences in platforms due to distance or water mass differences. The spatial filter was set to exclude stations where the ships were more than 10 km apart or were in different surface water property classifications (for water mass classifications, see Siegel et al., 2021) at the time of the cast. This spatial filtering procedure restricted the spatial comparison dataset to samples collected in surface water property classification and to the top 110 m of the water column where the Process Ship focused its sampling efforts. The spatial filtering procedure does not result in a dataset of direct comparisons because casts were not necessarily collected at the same time, but it does exclude any sampling when the ships were very distant. To allow direct comparison, we binned data at 10 m depth intervals, starting at 2 m, to most appropriately match the depth distribution of Niskin sampling.

The results of the spatial filtering for the Survey Ship non-optics casts are shown in **Figure 9A–C** (green circles). As suggested by initial comparison of the optics and non-

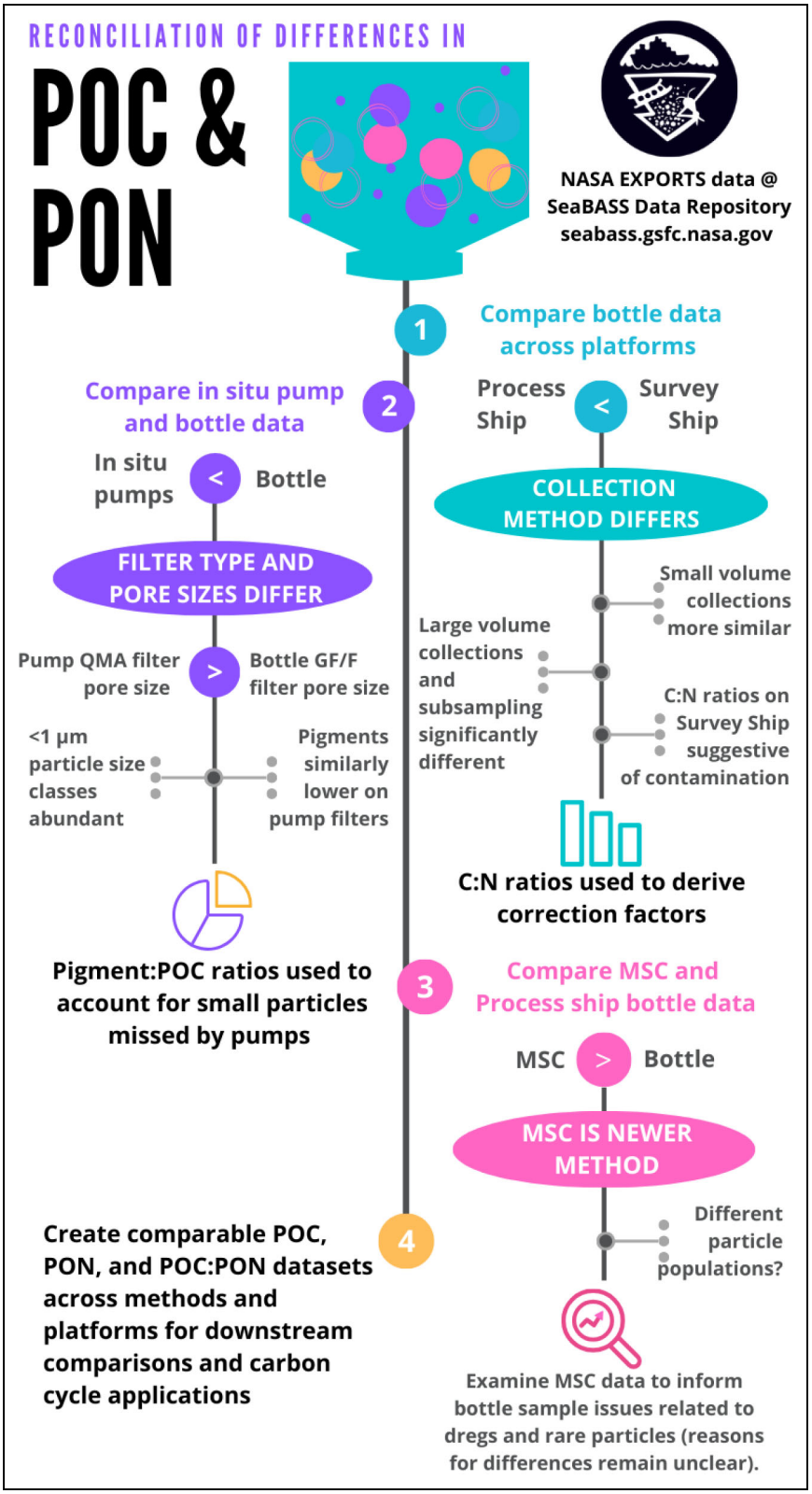


**Figure 7. Roadmap for reconciling differences in particulate organic carbon and nitrogen collected from multiple platforms.** This diagram represents the discussions and reconciliation process used to explore complementary datasets and their methods with varying degrees of disparity for determining particulate organic carbon (POC) and particulate nitrogen (PN), including from Marine Snow Catchers (MSC), during the NASA EXPORTS field program in the North Pacific Ocean.

optics casts, the Survey Ship and Process Ship data were much closer than in the non-spatially filtered dataset. In fact, the PN data were very similar (green versus purple circles in **Figure 9B**), suggesting no correction was required. The POC data of the Survey Ship optics casts were still higher than the Process Ship (**Figure 9A**), and

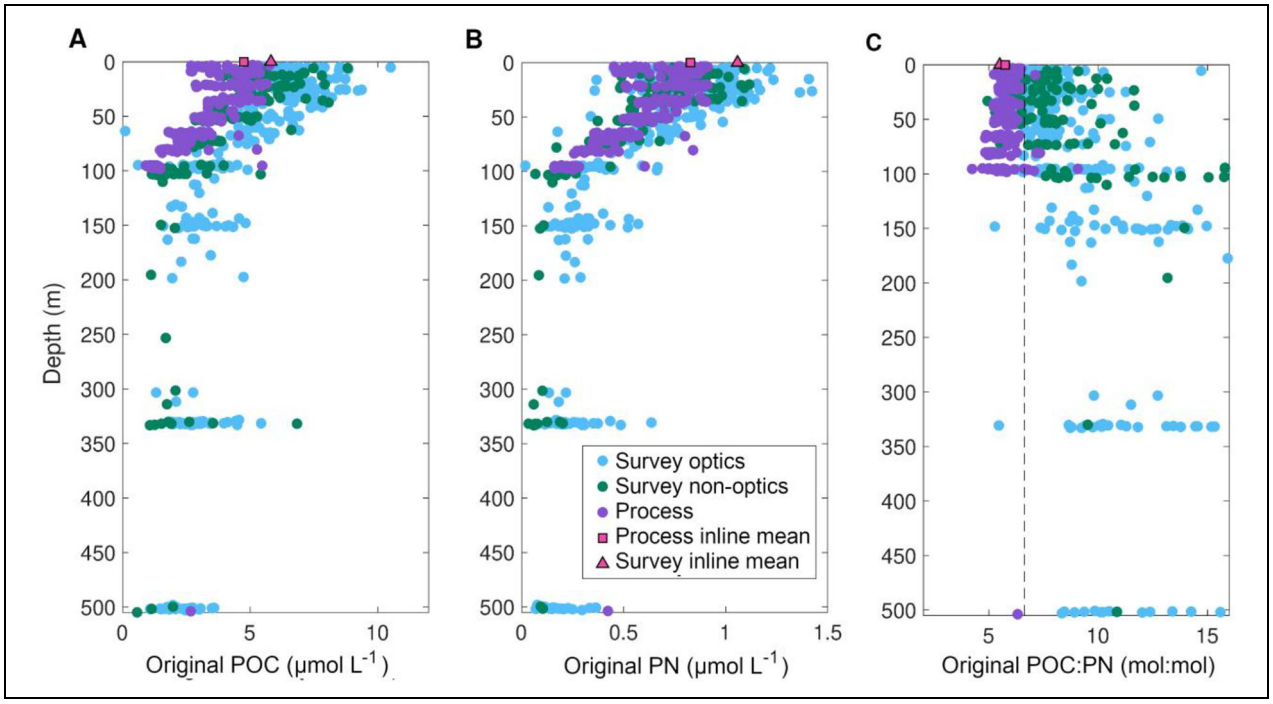


**Figure 8. Depth profiles of particulate organic carbon and particulate nitrogen separated by optics and non-optics casts.** Concentrations (μmol $L^{-1}$) of (A) particulate organic carbon (POC) and (B) particulate nitrogen (PN) and ratios of (C) POC:PN (mol:mol) are shown to a depth of 500 m, with optics (light blue) and non-optics (green) casts from the Survey Ship identified accordingly. Optics casts consisted of large volume collections from Niskin bottles into 20 L carboys and homogenization prior to subsampling into smaller Nalgene bottles, whereas non-optics casts collected small volumes (approximately 2 L) and were filtered directly from collection bottles. Mean values for Survey and Process ship inline measurements are also included (red). "Original" refers to POC and PN datasets after the initial blank correction (**Figure 2**) but before additional analyses and corrections to Survey Ship datasets.

the survey POC:PN data were consistently higher and increased with depth (**Figure 9C**) as the absolute values declined, suggesting a small additional POC blank correction would be appropriate for non-optics survey ship values.

To calculate the additional POC blank (*dC*) for the Survey Ship non-optics POC data, we used the Process Ship data as a POC:PN reference value:

$$\frac{(\overline{\mathrm{POC}} - \mathrm{dC})}{\overline{\mathrm{PON}}} = \mathrm{C} : \mathrm{N}_{\mathrm{ref}} \qquad (2)$$

where $\overline{\mathrm{POC}}$ and $\overline{\mathrm{PON}}$ are the average Survey Ship non-optics values of POC and PN in the surface layer; and dC is the additional blank correction, which on average brings the POC:PN ratio to the reference POC:PN value ($C:N_{ref}$; **Table 3**). We tried both the Process Ship-computed surface mean POC:PN ratio (5.92) and the Redfield POC:PN ratio (106:16) as $C:N_{ref}$. Adjusted Survey Ship non-optics POC values using the *dC* computed in this fashion with the Process Ship average as the $C:N_{ref}$ is shown in **Figure 9D** (green circles). After correction, there is a closer match between adjusted survey ship non-optics data and the Process Ship POC profile and the POC:PN ratio (**Figure 9F**), and there is no depth increase in POC:PN ratio. Using the Redfield ratio as the target $C:N_{ref}$ produced similar, but smaller corrections (**Table 3**; data not shown), but Survey Ship POC:PN ratios at depths greater than 100 m still showed increases that suggested this correction was insufficient.

For the spatially filtered optics casts (light blue circles in **Figure 9**), both Survey Ship binned POC and PN were higher throughout the profile than the comparable Process Ship data. Equation 2 therefore could not be used to estimate the additional POC blank for the optics casts. PN on the optics and non-optics casts of the Survey Ship were similar (**Figure 8B**), so we computed the offset of PN separately as the difference between the mean binned PN on the matching Survey Ship and Process ship casts. The corrected PNs were used with Equation 2 to estimate the additional POC blank for the optics casts. Results of applying this analysis using the Process Ship $C:N_{ref}$ are shown in **Figure 9D–F** (light blue circles). Summarized values for the additional blank computations are shown in **Table 3**.

We applied the blank corrections (both the handling-specific and platform-specific blanks) computed from the spatially filtered data (**Table 3**) to the Survey Ship POC and PN (**Figure 10A** and **B**, compare to **Figure 8A** and **B**), based on cast type, and computed corrected datasets (**Figure 10A–C**). Still apparent from these datasets is that the Survey Ship POC (**Figure 10A**) and POC:PN (**Figure 10C**) data are noisier than the corresponding Process Ship data, particularly at depth, but that ratios in particular are in better agreement despite higher

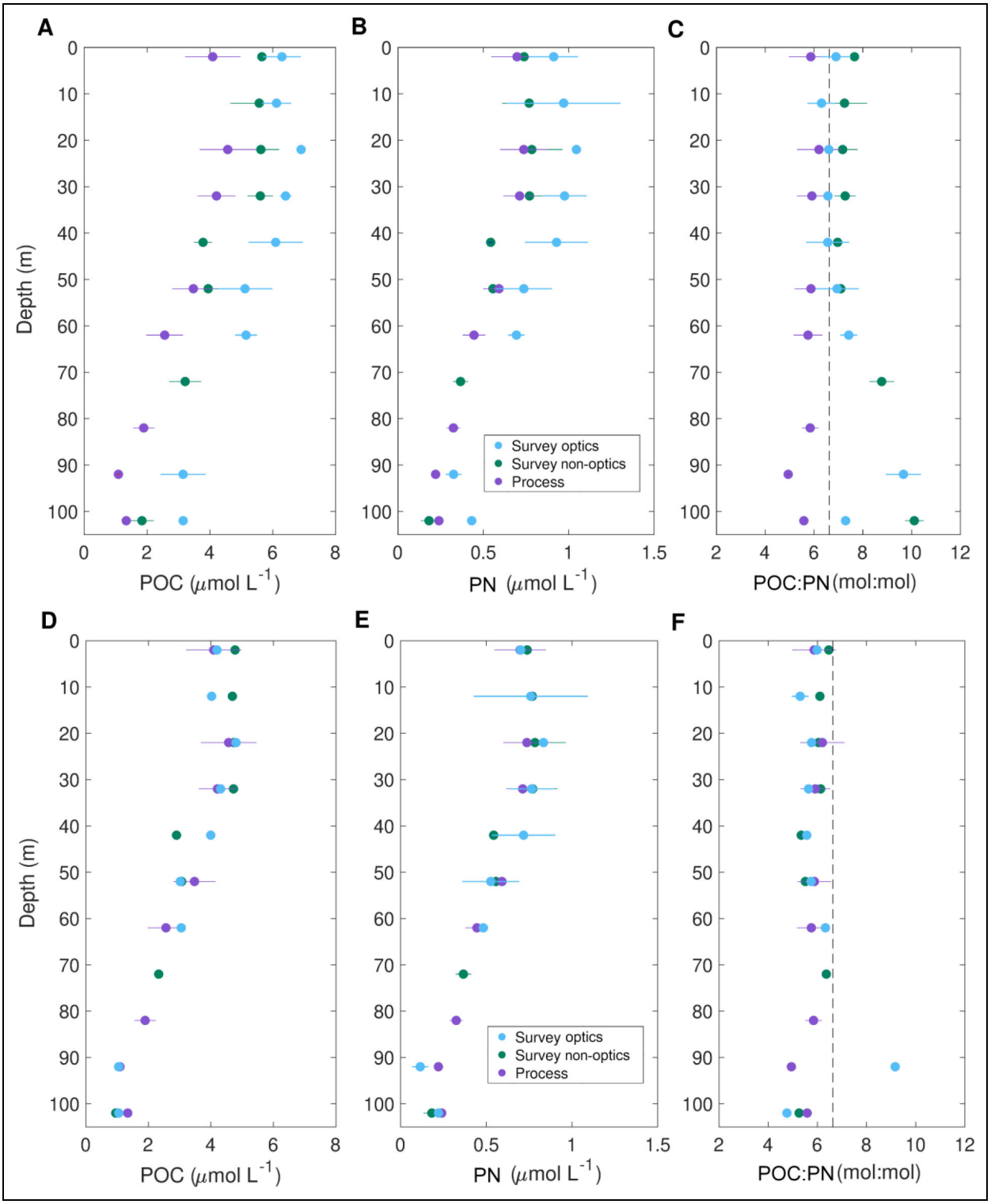


**Figure 9. Depth profiles of particulate organic carbon and particulate nitrogen before and after spatial filtering and correction.** Mean concentrations (μmol $L^{-1}$) of (A) particulate organic carbon (POC) and (B) particulate nitrogen (PN) and ratios of (C) POC:PN (mol:mol) are shown along with the corrected values for (D) POC, (E) PN, and (F) POC:PN from the NASA EXPORTS Survey Ship optics and non-optics casts and the Process Ship casts. Data are from casts where ships were in the same surface water property classification and separated by 10 km or less, limiting the data to a depth of approximately 100 m and surface water property classification 2 (Siegel et al., 2021). Error bars are standard deviations from 10 m bins starting at 2 m in order to better match the bottle trip depths.

variability. As with the initial statistical comparison of the two datasets, the analysis is restricted to samples collected above 110 m due to limited sampling below that depth by the Process Ship. Kolmogorov-Smirnov tests indicated that the ships' datasets were more similar for POC (Matlab, kstest2, $p = 0.047$) and also appear to have similar distributions for PN (Matlab, kstest2, $p = 0.44$). Cumulative distribution plots of the POC and PN datasets for the Process Ship and corrected Survey Ship can be found in Supplemental Figure S2.

In summary, we were able to arrive at plausible additional blank corrections for the Survey Ship POC and PN data based on spatially filtered data, with separate corrections for the "optics" and "non-optics" casts, which appear to display different levels of non-target carbon. The non-optics POC data were higher than the Process Ship, even in the spatially filtered dataset, but the PN agreed well. For the optics-associated casts, where the sample handling differed significantly from the Process Ship protocol, both POC and PN were affected, with molar POC:PN ratios sometimes exceeding 10. One possibility that could explain this result is the offset due to renewed sample homogenization and subsampling, due to the formation and subsequent collection of transparent exopolymer particles (TEP; Passow, 2000), which can result from agitation of phytoplankton cultures or natural seawater samples. However, subtracting the non-optics correction from the optics cast data, the molar ratio of the optics POC and PN after corrections is 7.05, which is much closer to the Redfield ratio (6.6) than to the POC:PN ratio of transparent exopolymer particles produced by phytoplankton in culture (approximately 25; Engel and Passow, 2001; Mari et al., 2001), which would have required a significantly different correction if TEP were a major reason for the offset. Thus, TEP formation resulting from sample handling was not a likely cause for this offset or only contributed marginally to any differences between methods. Additional insights are not available from documented handling procedures or other sources.

Spatial filtering of inline surface water datasets using the restrictions applied to the bottle casts resulted in only one sample from each ship that could be compared. In lieu of spatial filtering, statistical outliers within each ship's dataset were identified (Matlab, rmsoutliers) and removed. Mean values for POC and PN from the ships were then more similar (POC = 5.0 μmol $L^{-1}$ and 5.4 μmol $L^{-1}$ and PN = 0.84 μmol $L^{-1}$ and 0.98 μmol $L^{-1}$ for the

**Table 3. NASA EXPORTS particulate organic carbon and particulate nitrogen additional blank corrections (μg)**

| Correction[a] | Non-Optics | Optics |
|---|---|---|
| dC (Redfield) | 0.531 | 1.874 |
| dN (Redfield) | 0.000 | 0.211 |
| dC (Process Ship) | 0.882 | 2.098 |
| dN (Process Ship) | 0.000 | 0.211 |

[a]Survey ship corrections were determined from spatially filtered, binned data using the Redfield ratio or the Process Ship mixed layer POC:PN average, specific for Survey Ship optics casts and non-optics-associated CTD rosette casts.

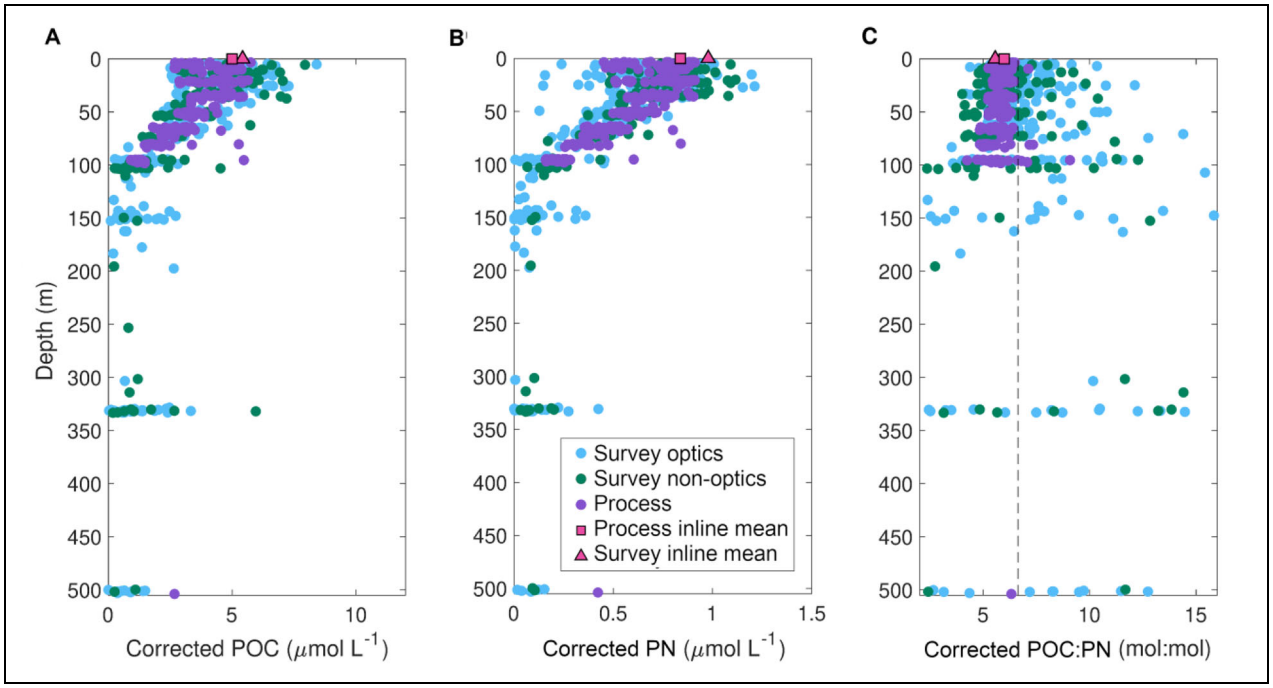


**Figure 10. Depth profiles of particulate organic carbon and particulate nitrogen after corrections.** Concentrations (μmol $L^{-1}$) of (A) particulate organic carbon (POC) and (B) particulate nitrogen (PN) and ratios of (C) POC:PN (mol:mol) are shown from the surface to a depth of 500 m (compare to **Figure 8A–C**). Blank-corrected Process Ship data plus additional corrections for the Survey Ship used corresponding factors from **Table 3** explicit for optics and non-optics casts. Inline data were corrected by applying the same correction as non-optics casts.

Process (n = 11) and Survey (n = 20) ships, respectively). A Kolmogorov-Smirnov test of the inline datasets with outliers removed indicated that the two datasets were from the same distribution for POC (p = 0.07) but less likely for PN (p = 0.02) in contrast to the datasets prior to outlier removal (POC, p = 0.03; PN, p = 0.01), which would suggest that neither POC nor PN were from the same distribution. The limited number of data points and the general agreement in values within the larger EXPORTS dataset suggested that additional consideration of these differences is not critical.

These results suggest that there might have been two separate impacts that resulted in an underestimation of the blanks for the Survey Ship casts. The first applies to all casts and affects only the POC data, while the second is restricted to the optics casts and affects both POC and PN with an average molar ratio of about 7. The POC offset that applies to both the Survey Ship's optics and non-optics casts (**Table 3**) argues for a possible hydrocarbon, plastic, or other carbon-rich contaminant that is unique to the Survey Ship (R/V *Sally Ride*). While no direct evidence from sample analysis is available to support the hydrocarbon hypothesis, aside from elevated C:N ratios, the rosette sampling area on the Survey Ship is adjacent to a cluster of fuel and/or lubricant tank vents and was documented photographically on a subsequent cruise (Figure S3). Fumes from these vents were reported as a problem on deck and in the labs by the science party during the EXPORTS North Pacific campaign. An improvised passive "fume hood" was installed by the ship's personnel during the cruise in an attempt to mitigate fumes directly reaching the rosette, suggesting a previous long-term exposure of the rosette and Niskin bottles to hydrocarbon emissions. No obvious contamination of DOC samples was observed on either ship on the EXPORTS field campaign (C Carlson and D Hansell, personal communication, 2020). DOC sampling involved smaller overall volumes (e.g., 40 mL) filtered directly from the Niskin bottle with high total carbon concentrations, while POC sampling involved collecting into secondary containers and filtering multiple liters of sample, which provided ample opportunity for sample and filter contamination, thus impacting lower target POC concentrations.

#### 4.1.2. In situ pumps and Niskin bottles (Step 2 in Figure 7)

In situ pump sampling resulted in substantially lower POC and PN compared to Niskin sampling at similar depths (**Figure 2A** and **B**) but did not deviate in the POC:PN ratio from the Process Ship determinations or from Redfield. Method comparisons indicated that filter choice could give rise to these differences if submicrometer particles were a significant component of POM. Niskin samples were collected onto pre-combusted GF/Fs with an estimated pore size of 0.3 μm after combustion (Nayar and Chou, 2003), while pumps collected particles approximately 1 μm and greater on pre-combusted QM-A filters and Nitex screens (**Table 1**). Multiple lines of evidence from supporting EXPORTS datasets indicate that small particles and phytoplankton were a significant component of POM and were missed by in situ pumps equipped with a single QM-A as the smallest filter.

PSDs, FCM, HPLC pigments and two pump PN samples collected from two depths on GF75 (0.3 μm nominal pore size) were used to evaluate the discrepancies between pumps and Niskin bottles. Size class estimates of POM using the VSF inversion technique suggest that submicrometer particles contributed about 35% of the total POM during EXPORTS, with little variability throughout the water column (**Figure 5A**). Analysis of Zea, a pigment largely diagnostic for picophytoplankton including small cyanobacteria like *Synechococcus* (0.43–1.76 μm; reviewed in Haëntjens et al., 2022), revealed that pump QM-A samples consistently undersampled this pigment, with the greatest difference found (only 14% of Niskin concentrations) in samples collected between 45 m and 55 m (**Figures 3B** and **4**) where *Synechococcus* had a subsurface peak in abundance (**Figure 5B**). Other pigments (Fuco and Perid, considered as diagnostic pigments for diatoms and dinoflagellates, respectively) were also undersampled on pump QM-A filters relative to bottle samples (**Figures 3C**, **D**, and **4**), but to a lesser extent, as would be expected as these are marker pigments for larger phytoplankton classes (e.g., Vidussi et al., 2001; Kramer and Siegel, 2019) and pump pigment data were restricted to the 1–5 μm fraction. Lastly, pump samples collected using 0.3 μm GF75 filters suggested that approximately 20%–30% of POC could be attributed to submicrometer particles within the euphotic zone, similar to the other, independent estimates. These observations combined suggest that discrepancies between in situ pump and Niskin POC and PN data can be attributed largely to filter choices and the associated pore size of those filters.

As such, we re-examined the pump POC data from 50 m in an attempt to account for the fraction of particles that were presumably too small to be captured by QM-A filters and to reconcile the dataset with bottle POC. We used three different methods in which we evaluated HPLC pigment concentrations measured from the Niskin and pump collections on the Survey Ship at the same four stations and the Process Ship POC data (**Figure 11**). The details of each individual matchup are provided in Table S1 and the average differences are reported below.

The first approach consisted of multiplying the difference in Tchla between bottle and pump samples from the Survey Ship (34% ± 9%, n = 4) by the POC:Tchla (μg:μg) ratio determined from the samples collected at 45–55 m depth from the Process Ship (163 ± 32, n = 22). This step results in an average adjusted pump POC of 2.5 ± 0.8 μmol $L^{-1}$, which is a factor of 1.4 lower than the average Process Ship bottle POC. The same POC:Tchla correction was applied in the second method, except that the average fraction of Tchla on the >5 μm size class (28% ± 5%, n = 3; Meyer et al., 2022) was subtracted from the Tchla concentration from the Survey Ship bottle samples. As such, the comparison of Tchla between bottle and pump samples was restricted to the <5 μm size class. This approach results in an average adjusted pump POC of 1.7 ± 0.5 μmol $L^{-1}$, which is still lower than the average Process Ship bottle POC by a factor of 2. Finally, we used

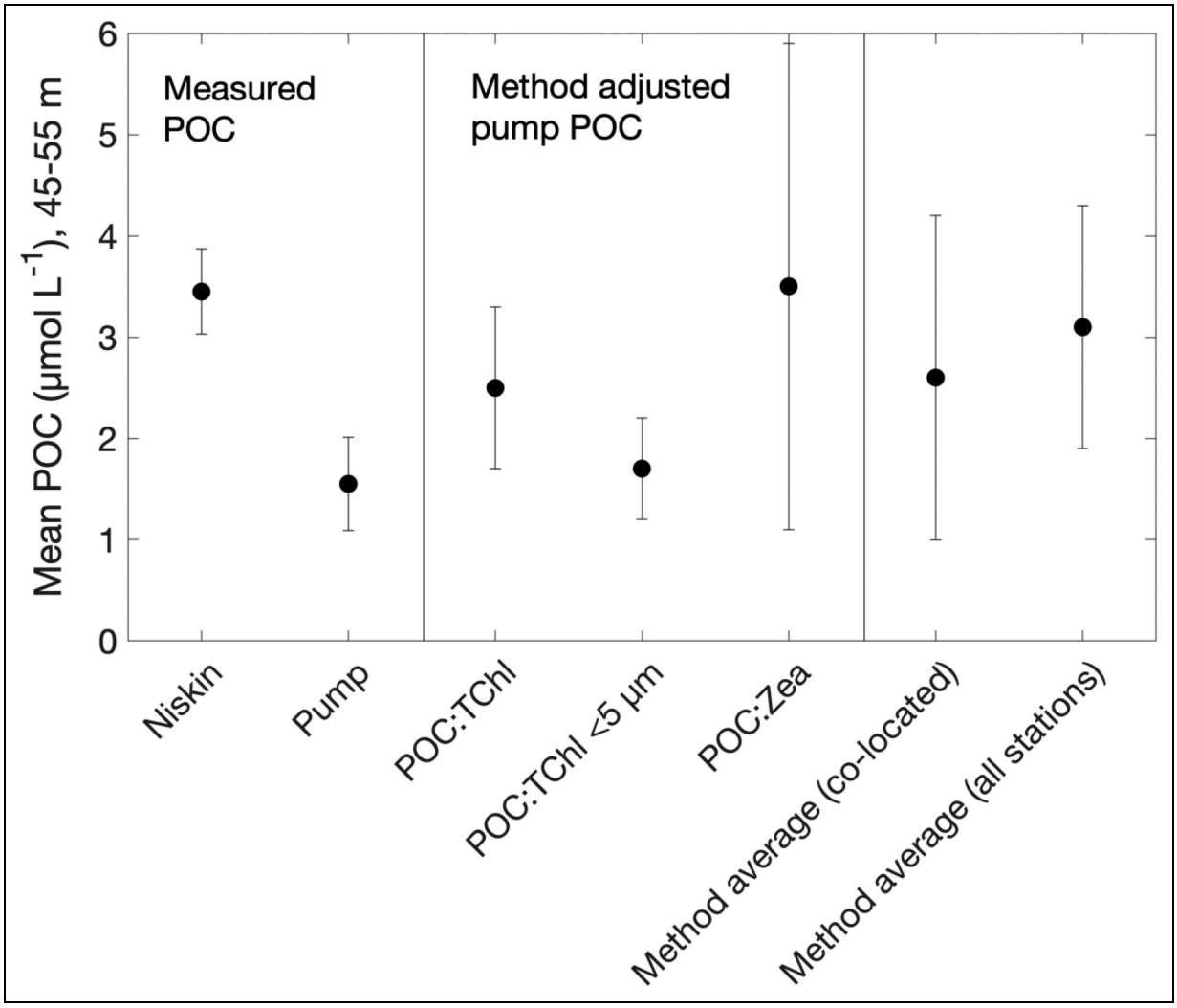


**Figure 11. Comparison of particulate organic carbon from Niskin bottles, in situ pumps and method-adjusted pump data.** Particulate organic carbon (POC) data from Process Ship Niskin bottles are compared with the in situ pump data from depths of 45–55 m and adjusted pump data using POC-to-pigment ratios from co-located pump and Niskin bottle HPLC pigment data for the average of co-located samples or the cruise average for all stations. Analysis was limited to total chlorophyll-*a* (TChla), <5 µm TChla, and zeaxanthin (Zea). Error bars are ±1 standard deviation. Additional information on adjusted pump data can be found in Table S1.

the difference in Zea observed between bottle and pump samples on the Survey Ship (65% ± 25%, n = 4) and the POC:Zea (µg:µg) ratio determined at 45–55 m depth from the Process Ship bottles (3174 ± 1341, n = 22). This ratio approach was chosen because the contribution of picophytoplankton to total POC biomass is better represented by Zea than by bulk Tchla in this dataset. Additionally, Zea was the pigment most undersampled by pump collections of the four pigments used in this analysis. This calculation resulted in an average adjusted pump POC of 3.5 ± 2.4 µmol $L^{-1}$, which is comparable to the average Process Ship bottle POC (**Figure 11**).

Each of these estimates has its limitations, including the fact that CTD and pump casts were not always conducted on the same day or time of day (Figure S4), which has been found in other studies to be important in POC determinations (Bishop et al., 1999), and that the assumption of constant POC:Tchla and POC:Zea ratios across stations and particle size ranges may not be correct. However, a comparison between ships for time of sampling for profiles or inline sampling shows relatively good agreement (Figure S4) and, despite the variability among methods and between stations (Table S1), the combination of three methods results in an average adjusted pump POC of 2.6 ± 1.6 µmol $L^{-1}$ that is more like concentrations encountered in the bottle samples (Niskin:pump = 1.3). When all the pigment data available from Survey Ship bottles and pumps are used (not just these 4 stations), a similar adjusted pump POC average is reached (3.1 ± 1.2 µmol $L^{-1}$; Table S1).

Taken together, these analyses suggest that the POC difference found between bottles and pumps is mostly due to the fact that pumps did not capture submicrometer particles given the larger pore size of the QM-A filters. This finding is consistent with the independent optical estimate that the 0.2–1.0 µm particle size class contributed 33% ± 6% of total POM at 50 m during EXPORTS (**Figure 5A**). From 100 to 500 m, making a similar

assessment is more difficult due to the low concentrations, often close to or below the limit of detection, of pigments. However, VSF inversion size class estimates of POM indicate that on average 24%–41% of total POM corresponded to the 0.2–1.0 μm size class at the pump depths between 100 m and 500 m. This result suggests that pumps still may miss the smaller sized particles at these depths, even though total POC concentrations for all size fractions decrease.

Follow-up filter comparison studies were undertaken on subsequent cruises. The first set of results was reported at the Ocean Sciences Meeting in 2022 (Creed and Lam, 2022), with results similar to this study across filter types applied to the same filtration approach. The second study was conducted during the EXPORTS field campaign in the North Atlantic Ocean in 2021. Filtrates from shipboard filtrations of whole seawater from multiple depths using pre-combusted (450°C, 4 hours) 25 mm Whatman® GF/F and QM-A filters were analyzed via FCM. Preliminary results indicate that QM-A filters do not capture a significant fraction of the phytoplankton community, including larger cells, relative to GF/F filters (Figure S5). These results, while not exhaustive, provide supporting evidence for the observed differences between in situ pumps and Niskin sampling regarding phytoplankton pigments and POC and PN during the EXPORTS field campaign in the North Pacific.

Factors that could not be addressed adequately for comparing pumps and Niskin bottles include zooplankton in samples; the extent to which particles pass through screens and QM-A filters due to breaking, orientation, or pressure; and inefficient rinsing of particles off screens. Potential loss of POM related to pressure differential across the filters during in situ pumping (Gardner et al., 2003) likely would have had a greater impact at 50 m given the higher particle loads and, as a result, lower flow rates reached during pumping at this depth compared to deeper waters. Yet, the relative discrepancy between bottles and pumps was similar at 50 and 100 m. Regarding the screen rinsing, assuming a maximum loss of 20% of POC and PN of >5 μm particles retained on the screen due to insufficient rinsing, and as seen in other studies (Buesseler et al., 1998), the discrepancy between bottles and pumps would still remain, as total POC would change by <0.02 μmol $L^{-1}$.

#### 4.1.3. Marine Snow Catchers and Niskins (Step 3 in Figure 7)

Concentrations of POC determined from the MSC T0 samples and the Process Ship Niskin bottles should be equal on average, because the POC analysis protocol (filter type and elemental analysis) was the same and samples were collected onboard the same vessel. A direct comparison between samples collected within a depth of less than 14 m and within fewer than 5 hours of each other and at the same station ($n = 19$) shows that the POC measured in the MSC T0 samples were on average 1.1 ± 0.9 μmol $L^{-1}$ higher that the Niskin POC values. When comparing the concentrations of POC measured from the same MSCs but in the suspended particle fraction (particles that did not reach the base of the MSC within the 2-hour settling time) with the POC measured in the Niskin bottles, the difference decreases to an average of 0.6 ± 1.3 μmol $L^{-1}$ ($n = 18$). The discrepancy between the MSC and the Niskin bottle appears to be smaller when POC values from the Niskin bottles are compared to suspended POC values from the MSC. This observation may imply a loss of sinking particles in Niskin bottle samples. Given that the time difference between when a Niskin is closed and when the sample is drawn was on the order of an hour or more (depending on the collection depth), a reasonable assumption is that, at least partially, sinking particles were below the spigot, the so-called "dregs," and thus were not sampled representatively (Gardner, 1977; Gardner et al., 2003). Data from the MSC indicate that in the upper 110 m, on average, 0.4 μmol $L^{-1}$ POC sank at an average sinking velocity of at least 18 m $day^{-1}$. If we considered that the height of the Niskin bottles was 1.06 m, particles with this sinking velocity would have settled below the spigot after less than 1.4 hours of settling. This evidence suggests that dregs may provide a partial explanation for the discrepancy.

In addition, the POC concentration measured from the MSC handling blank was approximately the same as the average intercept blank derived from the Niskins. The MSC handling blank likely was not a full adsorption blank as only 5 mL were filtered, suggesting that the true MSC blank should have been slightly higher than the Niskin blank, which includes the absorption of non-target DOC. The POC measured with the MSC may thus, on average, slightly overestimate the concentration of POC. However, because the MSC and the CTD rosette were not co-deployed and the sample number for the comparison was small ($n = 19$), discrepancy due to spatiotemporal variability cannot be excluded. Although the difference between the MSC and Niskin POC may not be systematic, dregs and unaccounted DOC absorption could partially explain the observed discrepancy. The molar POPN values measured in the MSC T0 sample and suspended particle fraction are reasonable and in agreement with values encountered in samples collected from Process Ship Niskin bottles.

### *4.2. Optics and POC*

Optical proxies for POC are abundant in the literature and allow investigators to assess particulate carbon on temporal and spatial resolutions not possible through traditional sampling techniques. Here, the Process Ship and Survey Ship POC were compared with particulate beam attenuation and backscatter measurements. Although sampling occurs on the same cast, the timing of the bottle and optical sampling differs. POC is measured from Niskin samples collected on the upcast of the CTD rosette. In contrast, optical instruments are deployed at the base of the rosette to measure undisturbed waters during the downcast. During the upcast, significant variability can occur because the Niskin- and instrument-laden CTD rosette moving through the water column can induce turbulence that causes a wake to develop, or even particles to fragment, affecting optical measurements (see, for example, the discussion in Cetinić et al., 2012). In

addition, for the Process Ship a significant decrease in beam attenuation was present in virtually every cast between 200 m and 400 m, rendering uncertainty in the optical upcast measurements. For these reasons, POC samples from the upcast were compared with optical measurements on the downcast on the same isopycnal. Prior to comparison, optical measurements of $c_p$ and $b_{bp}$ were also filtered using a 7-point running median to remove spikes present in the data. A total least squares regression, which considers errors and standard uncertainties in both variables (Boggs et al., 1987) was performed between the corrected POC values and either $c_p$ or $b_{bp}$ using measurements collected within the upper 100 m, after eliminating values with z-scores greater than 3 (i.e., samples more than 3 standard deviations away from the best-fit line; **Figure 12**).

The best-fit slope for Process Ship $c_p$ and POC was 33.4 ± 1.0 (µmol $L^{-1}$ m), with $r^2 = 0.89$ (n = 125), and for the corrected Survey Ship POC was 31.9 ± 1.5, with $r^2 = 0.66$ (n = 255; for the uncorrected POC data the Survey Ship slope was shallower at 27.7 ± 2.0, with overall greater variance, $r^2 = 0.46$). These slopes are within one standard deviation of each other, showing that once POC data were corrected for the Survey Ship Niskin samples, the two datasets agree. A fit for combined ship data results in a slope of 32.3 ± 1.1 with $r^2 = 0.72$ (n = 350). For $b_{bp}$, the best-fit slope for the Process Ship POC was 4114 ± 219 (µmol $L^{-1}$ m), with $r^2 = 0.70$ (n = 130), and for the corrected Survey Ship POC was 4122 ± 227, with $r^2 = 0.54$ (n = 263; again, before correction the slope for the Survey Ship was significantly shallower; 3690 ± 267, $r^2 = 0.40$). As with the relationship to $c_p$, once the Survey Ship POC data were corrected, the POC:$b_{bp}$ slopes agree well with each other. A fit for combined ship data results in a slope of 4068 ± 177, with $r^2 = 0.56$ (n = 393).

The literature abounds with multiple relationships for quantifying POC concentrations from $c_p$ and $b_{bp}$ (e.g., Bishop, 1999; Stramski et al., 2008; Cetinić et al., 2012; Boss et al., 2015; Graff et al., 2015). Cetinić et al. (2012; **Tables 1** and **2**) compiled relationships of $c_p$ and $b_{bp}$ with POC from commonly cited sources showing that the linear fit slopes of the relationships with $c_p$ range from 20.9 to 48.7 and for $b_{bp}$ from 2950 to 4464. The regression with $c_p$ found here (32.3 ± 1.1, for both ships) is similar to those calculated by Cetinić et al. (2012) for the North Atlantic springtime bloom (32.5) and Graff et al. (2015) from a north–south transect of the Atlantic Ocean (34.9). The regression measured here with respect to $b_{bp}$ of 4068 ± 177 lies between the slope calculated by Cetinić et al. (2012) of 2952 ± 146 (µmol $L^{-1}$ m) and that calculated by Stramski et al. (2008) of 4464 and is remarkably close to the POC:$b_{bp}$ relationship of 4064 reported by Graff et al. (2015).

Differences in relationships between optical parameters and POC can be attributed to sampling specifics such as optical instruments and calibrations, wavelengths, and measurement platforms, as well as POC collection and handling techniques. Additionally, differences in the observed relationships can be attributed to the natural variability driven by the particle dynamics and associated optical patterns. For example, Cetinić et al. (2012) found a significant decrease in the slope of $b_{bp}$ versus POC (from 3610 to 2950 µmol $L^{-1}$ m) when fit against downcast versus upcast CTD rosette measurements, and suggested that this finding was due to the break-up of particles during the CTD upcast, leading to an apparent decrease in $b_{bp}$. Similar discrepancies were found between upcast

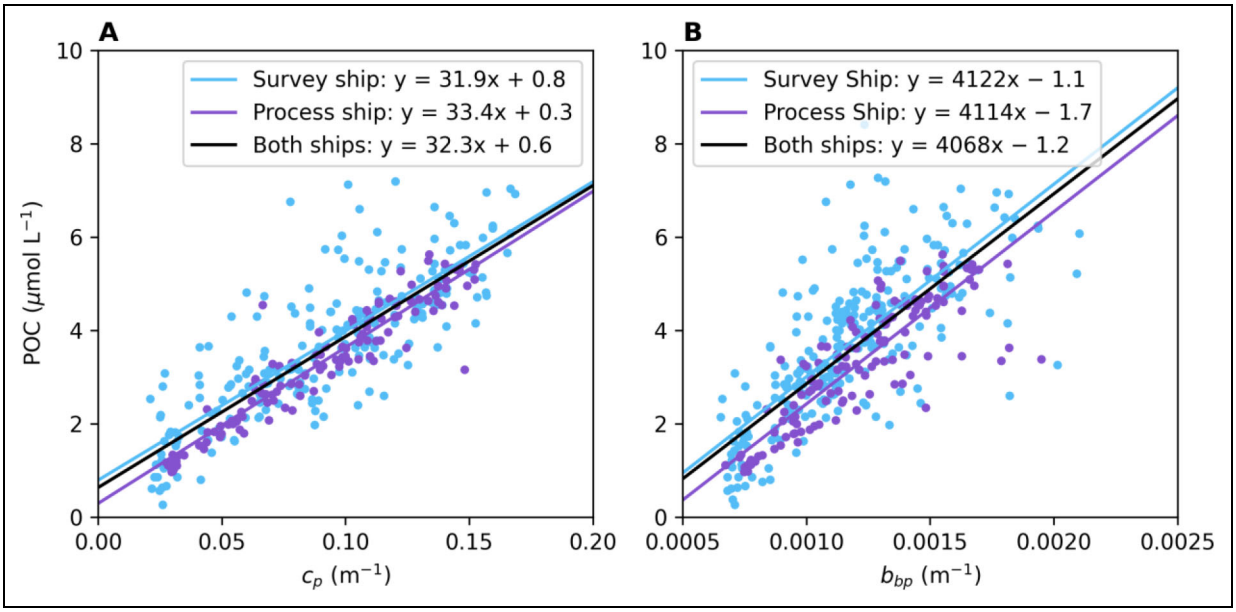


**Figure 12. Relationships of particulate organic carbon with beam attenuation and particulate backscattering.** Particulate organic carbon (POC) relationships with (A) particulate beam attenuation ($c_p$) and (B) backscattering ($b_{bp}$) are based on Process and Survey Ship Niskin POC datasets before and after corrections were applied. Lines indicate a total least squares regression analysis.

and downcast CTD rosette measurements on the Process Ship but not the Survey Ship in the North Pacific. At this time, we can only speculate as to why differences between downcast and upcast data were observed on one platform and not the other; possibilities include rosette hydrodynamics, spatial differences in sampling and particle characteristics, instrument-specific responses to environmental parameters (pressure, temperature, etc.) and bias due to specific placement on each platform relative to potential interference from other light sources. Understanding the relationships between optical properties and particle community characteristics are active areas of research that, in the future, will provide insights on the variability observed in these relationships.

## 5. Conclusions and recommendations

POC measurements, while critically important and commonly made, are fraught with operational differences in approaches for quantifying marine particles, as well as the potential for inaccuracies among collection or analysis methods. In our evaluation of the North Pacific EXPORTS POC (and PN) datasets, disparities were reconciled and understood only after considerations of stoichiometry, blanks, potential contamination issues, filter choices, phytoplankton pigment concentrations, particle size and community composition, and time-resolved measurements related to sinking particles and the dreaded dregs issue. It became clear that approaches for Niskin sampling, even when they were nearly identical, as in Process Ship, Survey Ship, Survey Ship optics and non-optics casts, could still lead to significant differences in measured POC and PN concentrations due to issues with the platform (suspected hydrocarbon contamination on the Survey Ship) and sample handling procedures (from delayed sampling and/or sample homogenization prior to dispensing). Planquette and Sherrell (2012) found that gentle mixing of the Go-Flo bottles used to collect water in situ before subsampling increased concentrations of some particulate elements by up to 50%. This effect was especially the case for lithogenic elements such as Al and Fe. Biogenic elements like P, which would be more likely to track with POC, showed a smaller difference, with up to 20% at the oligotrophic site and no significant difference at the coastal site, where settling of large particles would be expected to lead to greater differences between mixed and unmixed subsamples. At the time of sampling during this study in the North Pacific Ocean, total particle loads were low and dominated by smaller particles unlikely to sink rapidly in Niskin bottles and, thus, conditions were not likely to result in a large settling or dregs issue. The Survey Ship optics cast sampling from Niskin bottles did not include the collection of water below the spigot, and thus may not have actually captured the sinking particles that would result in higher POC and PN concentrations. The results of inline sampling from each ship, which would not have been subject to any dregs issues, suggest that these datasets were much more closely aligned than Niskin datasets from Survey and Process Ships. While we cannot exclude with absolute certainty the possibility that settling losses led to some of the observed discrepancies, sample handling procedures, supporting data and overall environmental conditions do not support the idea that settling was the cause of the initial discrepancies between Niskin sampling approaches.

Instead, stoichiometric ratios from the Survey Ship were high and highly variable, beyond expectations for oceanic environments. While POC:PN ratios will undoubtedly show variation over time and space, oceanic ratios are relatively constrained. Sterner et al. (2008) reported oceanic values ranging in mean values from 6.5 ($\pm$ 1.2) ($n = 159$, Indian Ocean) to 9.3 ($\pm$ 2.4) ($n = 30$, Sea of Japan), with their offshore oceanic regions having a median value of 6.6 (n, not reported). In our study, adjustments to Survey Ship datasets based on particle stoichiometry were required to align these measurements with the Process Ship dataset based on its consistent and reasonable stoichiometry (**Figure 10**). Efficacy of this correction was further confirmed by highly congruent relationships between the POC and particulate proxies.

In situ pumps using a single QM-A filter in this setting did not efficiently collect small phytoplankton and particles as evidenced by HPLC pigment data, modeled POM size fraction contributions, direct measurements, and phytoplankton community composition, all of which indicated the importance of submicrometer particles and small phytoplankton in this study. Adjusting in situ pump data using pigment ratios for the 45–55 m depth horizon indicated much better agreement with Niskin bottle data (**Figure 11**).

Lastly, MSCs provided insights on sinking particle dynamics and allowed an estimate of the potential consequences of missing sinking particles in Niskin sampling. The true MSC blanks were likely higher than those derived for the Niskin samples due to the more complex handling procedure of samples collected from the MSC and would have reduced differences observed between the approaches. Spatiotemporal differences in sampling also likely contributed to observed differences, and future studies dedicated to methodological comparisons could be helpful in discerning the extent of dregs issues across different environmental conditions.

Variability in datasets collected across different sampling platforms with distinct methodological approaches are highlighted when collocated in time and space. Yet these discrepancies, and the uncertainty they project into the data, will still be present when comparing datasets that are collected over different oceanic regions or time periods. Especially in waters with relatively low productivity, these discrepancies can be a significant fraction of the total signal.

The measurement reconciliation process to understand platform and method discrepancies in POC and PN measurements made clear that a broad suite of measurements and expertise was required to evaluate and understand the observed differences effectively. Recommendations for future studies, many of which are not new to the field and are similar to those provided by a recent community effort (Chaves et al., 2021), that we hope will benefit work in future collections and analyses of POC and PN samples are provided below.

First, adsorption blank measurements specific to each method and platform using pre-filtered natural seawater are important and need to be collected. Blanks that were not specific to the Survey Ship could not account for platform specific issues, possibly contamination, evidenced in stoichiometric ratios. More so, blanks covering the full range of depths would be most appropriate to account for differences in water chemistry and particle loads, which vary over time and space. The factors impacting adsorption blank magnitude and variability are not fully resolved but recognized as important for more accurate retrievals of particulate carbon concentrations (Cetinić et al., 2012; Graff et al., 2015; Novak et al., 2018). Collection and application of the filter blank is currently required for POC and PN submission to the NASA validation database (SeaBASS; Chaves et al., 2021), a community-imposed effort that hopefully will be accepted by other science databases. Second, filter choice is critical in analyses of particles and associated estimates of biomass. Even small differences in pore size (e.g., GF/F versus QM-A, or approximately 0.3 μm versus 1.0 μm, respectively) proved to be significant in this study of the North Pacific where submicrometer particles and small phytoplankton were abundant. As such, we recommend that a subset of samples be collected using filters with different pore sizes than are normally employed by a particular approach. Third, additional, independent variables should be measured using the same types of filters and filtration approaches that can help evaluate filter performance and or better understand what is being captured or lost. Here, HPLC pigments sampled from both in situ pump QM-A filters and collocated Niskin GF/F filters proved useful. Discrepancies between in situ pump data and bottle samples were also informed by other measurements (VSF inversions and FCM) related to particle and community size structure. Fourth, when contamination due to hydrocarbon or other non-target exposures are suspected, samples should be collected and reserved for specific analyses to address these concerns. Here, while the potential problem was identified at sea, no efforts were made to collect additional samples that would have allowed us to confirm or refute the suspected contaminant and its impact on the datasets.

The multitude of approaches used for the 2018 NASA EXPORTS field campaign to measure particulate matter resulted from funding of independent research groups and their unique scientific questions to address various aspects of particle export from the surface ocean and its relationship to other variables of interest. Each approach described above, with the exception of the MSC, has a substantial history of testing, field comparisons and issues regarding its application to collect and reflect particle stocks in the marine environment (Chaves et al., 2021). Differences between methods in this study, while not unexpected, offered an opportunity to compare across methods to try to understand why disparities existed across approaches and platforms. The results and comparison reported here do not provide conclusive results as to the most accurate approach for the study of marine particles. However, the lessons learned through the 2018 NASA EXPORTS experiment in the North Pacific and particle collection techniques were highly informative and hopefully will be applicable in future studies of ocean particles using similar approaches.

## Data accessibility statement

All datasets for this study can be found in the SeaWiFS Bio-optical Archive and Storage System (SeaBASS; https://seabass.gsfc.nasa.gov/cruise/EXPORTSNP) or EXPORTS 2018 BCO-DMO repository https://www.bco-dmo.org/program/757397.

## Supplemental files

The supplemental files for this article can be found as follows:

Supplemental material.docx

## Acknowledgments

The authors would like to thank NASA and NSF for logistical and financial support, the captains, crews, and marine technicians of the R/V *Revelle* and R/V *Ride*, chief scientists Norm Nelson, Mary Jane Perry, Debbie Steinberg and Jason Graff and additional members of the NASA EXPORTS Project Office for organizing the complexities of a multi-platform field campaign. Thanks to Adrian Marchetti and Meredith Meyer for size-fractionated chlorophyll data. The authors would like to acknowledge Steven Pike for his essential role in making the in situ pump deployments possible and Blaire P. Umhau for her work in processing pump filters at sea. The authors also would like to thank two reviewers whose insights and comments helped to clarify and improve the manuscript. This is PMEL Contribution Number 5421.

## Funding

JRG, JF, BV: NASA 80NSSC17K0568.

DAS, NBN, KB, SJK, UP, ER, JS, SH: NASA 80NSSC17K0692.

KOB, CBN, MRM: NASA 80NSSC17K0555, WHOI's Twilight Zone study (MRM, KOB), and the Ocean Frontier Institute International Postdoctoral Fellowship Program (MRM).

XZ, YX: NASA 80NSSC17K0656 and 80NSSC20K0350.

PL: NASA 80NSSC17K0555, NSF-OCE 1829614.

HGC: NSF 1830016.

CR, TC: NASA 80NSSC17K0700.

IC: NASA EXPORTS Project Office and NASA PACE Mission.

ZE: NASA Postdoctoral Program, administered by the Universities Space Research Association.

## Competing interests

The authors declare no competing interests.

## Author contributions

- Contributed to conception and design: JRG, NBN, SJK, IC, CR, KOB, DAS.
- Contributed to acquisition of data: JRG, NBN, MRM, SJK, UP, XZ, BV, HGC, JF, KB, PL, CBN, CR, TC, JS, SH, YX.

- Contributed to analysis and interpretation of data: JRG, ZE, NBN, KOB, MRM, ER, SJK, ZE, IC, UP, XZ, HGC, PL, CBN, YX.
- Drafted and/or revised the article: All authors.
- Approved the submitted version for publication: All authors.

## References


**Aas, E.** 1996. Refractive index of phytoplankton derived from its metabolite composition. *Journal of Plankton Research* **18**(12): 2223–2249. DOI: http://dx.doi.org/10.1093/plankt/18.12.2223.

**Babin, M**, **Morel, A**, **Fournier-Sicre, V**, **Fell, F**, **Stramski, D.** 2003. Light scattering properties of marine particles in coastal and open ocean waters as related to the particle mass concentration. *Limnology and Oceanography* **48**(2): 843–859. DOI: http://dx.doi.org/10.4319/lo.2003.48.2.0843.

**Bishop, JK.** 1999. Transmissometer measurement of POC. *Deep Sea Research Part I: Oceanographic Research Papers* **46**(2): 353–369. DOI: http://dx.doi.org/10.1016/S0967-0637(98)00069-7.

**Bishop, JK**, **Calvert, SE**, **Soon, MY.** 1999. Spatial and temporal variability of POC in the northeast Subarctic Pacific. *Deep Sea Research Part II: Topical Studies in Oceanography* **46**(11–12): 2699–2733. DOI: http://dx.doi.org/10.1016/S0967-0645(99)00081-8.

**Bishop, JKB**, **Edmond, JM.** 1976. A new large volume filtration system for the sampling of oceanic particulate matter. *Journal of Marine Research* **34**(1): 181–198.

**Bishop, JKB**, **Lam, PJ**, **Wood, TJ.** 2012. Getting good particles: Accurate sampling of particles by large volume in-situ filtration. *Limnology and Oceanography Methods* **10**(9): 681–710. DOI: http://dx.doi.org/10.4319/lom.2012.10.681.

**Bishop, JKB**, **Schupack, D**, **Sherrell, RM**, **Conte, M.** 1985. A multiple-unit large-volume in situ filtration system for sampling oceanic particulate matter in mesoscale environments. *Advances in Chemistry* **209**: 155–175. DOI: http://dx.doi.org/10.1021/ba-1985-0209.ch009.

**Boggs, PT**, **Byrd, RH**, **Schnabel, RB**. 1987. A stable and efficient algorithm for nonlinear orthogonal distance regression. *SIAM Journal on Scientific and Statistical Computing* **8**(6): 1052–1078. DOI: http://dx.doi.org/10.1137/0908085.

**Boss, E**, **Guidi, L**, **Richardson, MJ**, **Stemmann, L**, **Gardner, W**, **Bishop, JKB**, **Anderson, RF**, **Sherrell, RM.** 2015. Optical techniques for remote and in-situ characterization of particles pertinent to GEOTRACES. *Progress in Oceanography* **133**: 43–54. DOI: http://dx.doi.org/10.1016/j.pocean.2014.09.007.

**Boss, E**, **Haëntjens, N**, **Ackleson, S**, **Balch, B**, **Chase, A**, **Dall'Olmo, G**, **Freeman, S**, **Liu, Y**, **Loftin, J**, **Neary, W**, **Nelson, N**. 2019a. Ocean optics and biogeochemistry protocols for satellite ocean colour sensor validation, in Neeley, AR, Mannino, A eds., *Inherent optical property measurements and protocols: Best practices for the collection and processing of ship-based underway flow-through optical data*. Nova Scotia, Canada: International Ocean-Colour Coordinating Group (IOCCG): 22. (IOCCG Protocol Series; vol. 4.0). DOI: http://dx.doi.org/10.25607/OBP-664.

**Boss, E**, **Twardowski, M**, **McKee, D**, **Cetinić, I**, **Slade, W**. 2019b. Beam transmission and attenuation coefficients: Instruments, characterization, field measurements and data analysis protocols, in Neeley, A, Cetinić, I eds., *IOCCG ocean optics and biogeochemistry protocols for satellite ocean colour sensor validation*. Nova Scotia, Canada: IOCCG: 17. (IOCCG Protocol Series: vol. 2.0). DOI: http://dx.doi.org/10.25607/OBP-458.

**Boyd, PW**, **Claustre, H**, **Levy, M**, **Siegel, DA**, **Weber, T**. 2019. Multi-faceted particle pumps drive carbon sequestration in the ocean. *Nature* **568**(7752): 327–335. DOI: http://dx.doi.org/10.1038/s41586-019-1098-2.

**Buesseler, K**, **Ball, L**, **Andrews, J**, **Benitez-Nelson, C**, **Belastock, R**, **Chai, F**, **Chao, Y**. 1998. Upper ocean export of particulate organic carbon in the Arabian Sea derived from thorium-234. *Deep Sea Research Part II: Topical Studies in Oceanography* **45**(10–11): 2461–2487. DOI: http://dx.doi.org/10.1016/S0967-0645(98)80022-2.

**Buesseler, KO**, **Benitez-Nelson, CR**, **Roca-Martí, M**, **Wyatt, A**, **Resplandy, L**, **Clevenger, SJ**, **Drysdale, JA**, **Estapa, ML**, **Pike, S**, **Umhau, BP**. 2020. High-resolution spatial and temporal measurements of particulate organic carbon flux using thorium-234 in the northeast Pacific Ocean during the EXport Processes in the Ocean from RemoTe Sensing field campaign. *Elementa: Science of the Anthropocene* **8**(1): 030. DOI: http://dx.doi.org/10.1525/elementa.2020.030.

**Cetinić, I**, **Perry, MJ**, **Briggs, NT**, **Kallin, E**, **D'Asaro, EA**, **Lee, CM**. 2012. Particulate organic carbon and inherent optical properties during 2008 North Atlantic bloom experiment. *Journal of Geophysical Research: Oceans* **117**(C6): C06028. DOI: http://dx.doi.org/10.1029/2011JC007771.

**Chaves, JE**, **Cetinić, I**, **Dall'Olmo, G**, **Estapa, M**, **Gardner, W**, **Goñi, M**, **Graff, JR**, **Hernes, P**, **Lam, PJ**, **Liu, Z**, **Lomas, MW**, **Mannino, M**, **Novak, MG**, **Turnewitsch, R**, **Werdell, PJ**, **Westberry, TK**. 2021. *IOCCG ocean optics and biogeochemistry protocols for satellite ocean colour sensor validation: Particulate organic matter sampling and measurement protocols: Consensus towards future ocean color missions*. Nova Scotia, Canada: IOCCG: 54. (IOCCG Protocol Series vol. 6.0). DOI: http://dx.doi.org/10.25607/OBP-1646.

**Chavez, FP**, **Buck, KR**, **Bidigare, RR**, **Karl, DM**, **Hebel, D**, **Latasa, M**, **Campbell, L**, **Newton, J**. 1995. On the chlorophyll a retention properties of glass-fiber GF/F filters. *Limnology and Oceanography* **40**(2): 428–433. DOI: http://dx.doi.org/10.4319/lo.1995.40.2.0428.

**Creed, N**, **Lam, P**. 2022. Assessing bottle-pump differences in sampling for marine particulate organic carbon. Ocean Sciences Meeting.

**Dickson, ML**, **Wheeler, PA**. 1993. Chlorophyll a concentrations in the North Pacific: Does a latitudinal gradient exist? *Limnology and Oceanography* **38**(8): 1813–1818. DOI: http://dx.doi.org/10.4319/lo.1993.38.8.1813.

**Ehrhardt, M**, **Koeve, W**. 1999. Determination of particulate organic carbon and nitrogen, in Grasshoff, K, Kremling, K, Ehrhardt, M eds., *Methods of seawater analysis. 3rd ed.* Weinheim, Germany: Wiley: 437–444.

**Engel, A**, **Passow, U**. 2001. Carbon and nitrogen content of transparent exopolymer particles (TEP) in relation to their Alcian Blue adsorption. *Marine Ecology Progress Series* **219**: 1–10. DOI: http://dx.doi.org/10.3354/meps219001.

**Erickson, ZK**, **Cetinic, I**, **Zhang, X**, **Boss, E**, **Werdell, PJ**, **Freeman, S**, **Hu, L**, **Lee, C**, **Omand, M**, **Perry, MJ.** 2022. Alignment of optical backscatter measurements from the EXPORTS Northeast Pacific Field Deployment. *Elementa: Science of the Anthropocene* **10**(1): 00021. DOI: http://dx.doi.org/10.1525/elementa.2021.00021.

**EXPORTS NP Science Team**. 2021. EXPORTS measurements and protocols for the NE Pacific Campaign, edited by Cetinić, I, Soto-Ramos, I. Greenbelt, MD: NASA Goddard Space Flight Center. NASA/TM-20205007358.

**Gardner, WD**. 1977. Incomplete extraction of rapidly settling particles from water samplers. *Limnology and Oceanography* **22**(4): 764–768. DOI: https://doi.org/10.4319/lo.1977.22.4.0764.

**Gardner, WD**, **Mishonov, AV**, **Richardson, MJ**. 2006. Global POC concentrations from in-situ and satellite data. *Deep Sea Research Part II: Topical Studies in Oceanography* **53**(5–7): 718–740. DOI: http://dx.doi.org/10.1016/j.dsr2.2006.01.029.

**Gardner, WD**, **Richardson, MJ**, **Carlson, CA**, **Hansell, D**, **Mishonov, AV**. 2003. Determining true particulate organic carbon: Bottles, pumps and methodologies. *Deep Sea Research Part II: Topical Studies in Oceanography* **50**(3–4): 655–674. DOI: http://dx.doi.org/10.1016/S0967-0645(02)00589-1.

**Giering, SLC**, **Sanders, R**, **Martin, AP**, **Lindemann, C**, **Möller, KO**, **Daniels, CJ**, **Mayor, DJ**, **St. John, MA**. 2016. High export via small particles before the onset of the North Atlantic spring bloom. *Journal of Geophysical Research: Oceans* **121**(9): 6929–6945. DOI: http://dx.doi.org/10.1002/2016JC012048.

**Graff, JR**, **Behrenfeld, MJ**. 2018. Photoacclimation responses in subarctic Atlantic phytoplankton following a natural mixing-restratification event. *Frontiers in Marine Science* **5**: 209. DOI: http://dx.doi.org/10.3389/fmars.2018.00209.

**Graff, JR**, **Westberry, TK**, **Milligan, AJ**, **Brown, MB**, **Dall'Olmo, G**, **van Dongen-Vogels, V**, **Reifel, KM**, **Behrenfeld, MJ**. 2015. Analytical phytoplankton carbon measurements spanning diverse ecosystems. *Deep Sea Research Part I: Oceanographic Research Papers* **102**: 16–25. DOI: http://dx.doi.org/10.1016/j.dsr.2015.04.006.

**Haëntjens, N**, **Boss, ES**, **Graff, JR**, **Chase, AP, Karp-Boss, L**. 2022. Phytoplankton size distributions in the western North Atlantic and their seasonal variability. *Limnology and Oceanography* **67**(8): 1865–1878. DOI: https://doi.org/10.1002/lno.12172.

**Honjo, S**, **Dymond, J**, **Collier, R**, **Manganini, SJ**. 1995. Export production of particles to the interior of the equatorial Pacific Ocean during the 1992 EqPac experiment. *Deep Sea Research Part II: Topical Studies in Oceanography* **42**(2–3): 831–870. DOI: http://dx.doi.org/10.1016/0967-0645(95)00034-N.

**Hooker, SB**, **Clementson, L**, **Thomas, CS**, **Schlüter, L**, **Allerup, M**, **Ras, J**, **Claustre, H**, **Normandeau, C**, **Cullen, J**, **Kienast, M**, **Kolowski, W**. 2012. The Fifth SeaWiFS HPLC Analysis Round-Robin Experiment (SeaHARRE-5), NASA Technical Memorandum 2012-217503.

**Hu, L**, **Zhang, X**, **Perry, MJ**. 2019a. Light scattering by pure seawater: Effect of pressure. *Deep Sea Research Part I: Oceanographic Research Papers* **146**: 103–109. DOI: http://dx.doi.org/10.1016/j.dsr.2019.03.009.

**Hu, L**, **Zhang, X**, **Xiong, Y**, **He, MX**. 2019b. Calibration of the LISST-VSF to derive the volume scattering functions in clear waters. *Optics Express* **27**(16): A1188–A1206. DOI: http://dx.doi.org/10.1364/OE.27.0A1188.

**Jeffrey, S**, **Wright, S**, **Zapata, M**. 2011. Microalgal classes and their signature pigments, in Roy, S, Llewellyn, C, Egeland, E, Johnsen, G eds., *Phytoplankton pigments: Characterization, chemotaxonomy and applications in oceanography.* Cambridge, UK: Cambridge University Press: 3–77. (Cambridge Environmental Chemistry Series). DOI: http://dx.doi.org/10.1017/CBO9780511732263.004.

**Khelifa, A**, **Hill, PS.** 2006. Models for effective density and settling velocity of flocs. *Journal of Hydraulic Research* **44**(3): 390–401. DOI: http://dx.doi.org/10.1080/00221686.2006.9521690.

**Knap, AH**, **Michaels, A**, **Close, AR**, **Ducklow, H**, **Dickson, AG**. 1996. Protocols for the Joint Global Ocean Flux Study (JGOFS) core measurements. Paris, France: UNESCO-IOC. Intergovernmental Oceanographic Commission Manuals and Guides 29: 170. DOI: http://dx.doi.org/10.25607/OBP-1409.

**Kramer, SJ**, **Siegel, DA**. 2019. How can phytoplankton pigments be best used to characterize surface ocean phytoplankton groups for ocean color remote sensing algorithms? *Journal of Geophysical Research: Oceans* **124**(11): 7557–7574. DOI: http://dx.doi.org/10.1029/2019JC015604.

**Kramer, SJ**, **Siegel, DA**, **Graff, JR**. 2020. Phytoplankton community composition determined from covariability among phytoplankton pigments from the NAAMES field campaign. *Frontiers in Marine Science* **7**: 215. DOI: http://dx.doi.org/10.1029/2019JC015604.

**Lam, PJ**, **Ohnemus, DC**, **Auro, ME**. 2015. Size-fractionated major particle composition and concentrations from the US GEOTRACES North Atlantic Zonal Transect. *Deep Sea Research Part II: Topical Studies in Oceanography* **116**: 303–320. DOI: http://dx.doi.org/10.1016/j.dsr2.2014.11.020.

**Lampitt, RS**, **Wishner, KF**, **Turley, CM**, **Angel, MV**. 1993. Marine snow studies in the Northeast Atlantic Ocean: Distribution, composition and role as a food source for migrating plankton. *Marine Biology* **116**: 689–702. DOI: https://doi.org/10.1007/BF00355486.

**Liu, Z**, **Cochran, JK**, **Lee, C**, **Gasser, B**, **Miquel, JC**, **Wakeham, SG**. 2009. Further investigations on why POC concentrations differ in samples collected by Niskin bottle and in situ pump. *Deep Sea Research Part II: Topical Studies in Oceanography* **56**(18): 1558–1567. DOI: http://dx.doi.org/10.1016/j.dsr2.2008.12.019.

**Liu, Z**, **Stewart, G**, **Cochran, JK**, **Lee, C**, **Armstrong, RA**, **Hirschberg, DJ**, **Gasser, B**, **Miquel, JC**. 2005. Why do POC concentrations measured using Niskin bottle collections sometimes differ from those using in-situ pumps? *Deep Sea Research Part I: Oceanographic Research Papers* **52**(7): 1324–1344. DOI: http://dx.doi.org/10.1016/j.dsr.2005.02.005.

**Maiti, K**, **Buesseler, KO**, **Pike, SM**, **Benitez-Nelson, C**, **Cai, P**, **Chen, W**, **Cochran, K**, **Dai, M**, **Dehairs, F**, **Gasser, B**, **Kelly, RP**. 2012. Intercalibration studies of short-lived thorium-234 in the water column and marine particles. *Limnology and Oceanography: Methods* **10**(9): 631–644. DOI: http://dx.doi.org/10.4319/lom.2012.10.631.

**Mari, X**, **Beauvais, S**, **Lemée, R**, **Pedrotti, ML**. 2001. Non-Redfield C:N ratio of transparent exopolymeric particles in the northwestern Mediterranean Sea. *Limnology and Oceanography* **46**(7): 1831–1836. DOI: http://dx.doi.org/10.4319/lo.2001.46.7.1831.

**McNair, HM**, **Morison, F**, **Graff, JR**, **Rynearson, TA**, **Menden-Deuer, S.** 2021. Microzooplankton grazing constrains pathways of carbon export in the subarctic North Pacific. *Limnology and Oceanography* **66**: 2697–2711. DOI: http://dx.doi.org/10.1002/lno.11783.

**Menzel, DW**, **Vaccaro, RF**. 1964. The measurement of dissolved organic and particulate carbon in seawater. *Limnology and Oceanography* **9**(1): 138–142. DOI: http://dx.doi.org/10.4319/lo.1964.9.1.0138.

**Meyer, MG**, **Gong, W**, **Kafrissen, SM**, **Torano, O**, **Varela, DE**, **Santoro, AE**, **Cassar, N**, **Gifford, S**, **Niebergall, AK**, **Sharpe, G**, **Marchetti, A**. 2022. Phytoplankton size-class contributions to new and regenerated production during the EXPORTS Northeast Pacific Ocean field deployment. *Elementa: Science of the Anthropocene* **10**(1): 00068. DOI: http://dx.doi.org/10.1525/elementa.2021.00068.

**Moran, SB**, **Charette, MA**, **Pike, SM**, **Wicklund, CA**. 1999. Differences in seawater particulate organic carbon concentration in samples collected using small-and large-volume methods: The importance of DOC adsorption to the filter blank. *Marine Chemistry* **67**(1–2): 33–42. DOI: http://dx.doi.org/10.1016/S0304-4203(99)00047-X.

**Morel, A**, **Ahn, YH.** 1990. Optical efficiency factors of free-living marine bacteria: Influence of bacterioplankton upon the optical properties and particulate organic carbon in oceanic waters. *Journal of Marine Research* **48**: 145–175. DOI: http://dx.doi.org/10.1357/002224090784984632.

**Nayar, S**, **Chou, LM**. 2003. Relative efficiencies of different filters in retaining phytoplankton for pigment and productivity studies. *Estuarine, Coastal and Shelf Science* **58**(2): 241–248. DOI: http://dx.doi.org/10.1016/S0272-7714(03)00075-1.

**Novak, MG**, **Cetinić, I**, **Chaves, JE**, **Mannino, A**. 2018. The adsorption of dissolved organic carbon onto glass fiber filters and its effect on the measurement of particulate organic carbon: A laboratory and modeling exercise. *Limnology and Oceanography: Methods* **16**(6): 356–366. DOI: http://dx.doi.org/10.1002/lom3.10248.

**Passow, U**. 2000. Formation of transparent exopolymer particles, TEP, from dissolved precursor material. *Marine Ecology Progress Series* **192**: 1–11. DOI: http://dx.doi.org/10.3354/meps192001.

**Planquette, H**, **Sherrell, RM**. 2012. Sampling for particulate trace element determination using water sampling bottles: Methodology and comparison to in situ pumps. *Limnology and Oceanography: Methods* **10**(5): 367–388. DOI: http://dx.doi.org/10.4319/lom.2012.10.367.

**Riley, JS**, **Sanders, R**, **Marsay, C**, **Le Moigne, FA**, **Achterberg, EP**, **Poulton, AJ**. 2012. The relative contribution of fast and slow sinking particles to ocean carbon export. *Global Biogeochemical Cycles* **26**(1): GB1026. DOI: http://dx.doi.org/10.1029/2011GB004085.

**Roca-Martí, M**, **Benitez-Nelson, CR**, **Umhau, BP**, **Wyatt, AM**, **Clevenger, SJ**, **Pike, S**, **Horner, TJ**, **Estapa, ML**, **Resplandy, L**, **Buesseler, KO.** 2021. Concentrations, ratios, and sinking fluxes of major bioelements at Ocean Station Papa. *Elementa: Science of the Anthropocene* **9**(1): 00166. DOI: http://dx.doi.org/10.1525/elementa.2020.00166.

**Romanelli, E**, **Sweet, J**, **Giering, SLC**, **Siegel, D**, **Passow, U.** 2023. The presence of transparent exopolymer particles rather than ballast determines sinking of small particles during late summer in the Northeast Pacific Ocean. *Elementa: Science of the Anthropocene* **11**(1): 00122. DOI: https://doi.org/10.1525/elementa.2022.00122.

**Siegel, DA**, **Cetinić, I**, **Graff, JR**, **Lee, CM**, **Nelson, N**, **Perry, MJ**, **Soto Ramos, I**, **Steinberg, DK**, **Buesseler, K**, **Hamme, R**, **Fassbender, AJ**, **Nicholson, D**, **Omand, MM**, **Robert, M**, **Thompson, A**, **Amaral, V**, **Behrenfeld, M**, **Benitez-Nelson, C**, **Bisson, K**, **Boss, E**, **Boyd, PW**, **Brzezinski, M**, **Buck, K**, **Burd, A**, **Burns, S**, **Caprara, S**, **Carlson, C**, **Cassar, N**, **Close, H**, **D'Asaro, E**, **Durkin, C**, **Erickson, Z**, **Estapa, ML**, **Fields, E**, **Fox, J**, **Freeman, S**, **Gifford, S**, **Gong, W**, **Gray, D**, **Guidi, L**, **Haëntjens, N**, **Halsey, K**, **Huot, Y**, **Hansell, D**, **Jenkins, B**, **Karp-Boss,**

**L**, **Kramer, S**, **Lam, P**, **Lee, J-M**, **Maas, A**, **Marchal, O**, **Marchetti, A**, **McDonnell, A**, **McNair, H**, **Menden-Deuer, S**, **Morison, F**, **Niebergall, AK**, **Passow, U**, **Popp, B**, **Potvin, G**, **Resplandy, L**, **Roca-Martí, M**, **Roesler, C**, **Rynearson, T**, **Traylor, S**, **Santoro, A**, **Seraphin, KD**, **Sosik, HM**, **Stamieszkin, K**, **Stephens, B**, **Tang, W**, **Van Mooy, B**, **Xiong, Y**, **Zhang, X**. 2021. An operational overview of the EXport Processes in the Ocean from RemoTe Sensing (EXPORTS) Northeast Pacific field deployment. *Elementa: Science of the Anthropocene* **9**(1): 00107. DOI: http://dx.doi.org/10.1525/elementa.2020.00107.

**Sterner, RW**, **Andersen, T**, **Elser, JJ**, **Hessen, DO**, **Hood, JM**, **McCauley, E**, **Urabe, J.** 2008. Scale-dependent carbon:nitrogen:phosphorus seston stoichiometry in marine and freshwaters. *Limnology and Oceanography* **53**(3): 1169–1180. DOI: http://dx.doi.org/10.4319/lo.2008.53.3.1169.

**Stramski, D**, **Reynolds, RA**, **Babin, M**, **Kaczmarek, S**, **Lewis, MR**, **Röttgers, R**, **Sciandra, A, Stramska, M, Twardowski, MS, Franz, BA, Claustre, H.** 2008. Relationships between the surface concentration of particulate organic carbon and optical properties in the eastern South Pacific and eastern Atlantic Oceans. *Biogeosciences* **5**: 171–201. DOI: https://doi.org/10.5194/bg-5-171-2008.

**Twardowski, M**, **Zhang, X**, **Vagle, S**, **Sullivan, J**, **Freeman, S**, **Czerski, H**, **You, Y**, **Bi, L**, **Kattawar, G**. 2012. The optical volume scattering function in a surf zone inverted to derive sediment and bubble particle subpopulations. *Journal of Geophysical Research: Oceans* **117**(C7): C00H17. DOI: http://dx.doi.org/10.1029/2011JC007347.

**Van Heukelem, L**, **Hooker, SB**. 2011. The importance of a quality assurance plan for method validation and minimizing uncertainties in the HPLC analysis of phytoplankton pigments. *Phytoplankton Pigments* **5**: 195–256. DOI: http://dx.doi.org/10.1017/CBO9780511732263.009.

**Vidussi, F**, **Claustre, H**, **Manca, BB**, **Luchetta, A**, **Marty, JC.** 2001. Phytoplankton pigment distribution in relation to upper thermocline circulation in the eastern Mediterranean Sea during winter. *Journal of Geophysical Research: Oceans* **106**(C9): 19939–19956. DOI: http://dx.doi.org/10.1029/1999JC000308.

**Wilson, RF**. 1961. Measurement of organic carbon in sea water. *Limnology and Oceanography* **6**(3): 259–261. DOI: http://dx.doi.org/10.4319/lo.1961.6.3.0259.

**Wojtal, PK**, **Doherty, SC**, **Shea, CH**, **Popp, BN**, **Benitez-Nelson, CR**, **Buesseler, KO**, **Estapa, ML**, **Roca-Martí, M**, **Close, HG.** 2023. Deconvolving mechanisms of particle flux attenuation using nitrogen isotope analyses of amino acids. *Limnology and Oceanography* **68**(15): 1–17. DOI: http://dx.doi.org/10.1002/lno.12398.

**Zhang, X**, **Gray, DJ**, **Huot, Y**, **You, Y**, **Bi, L**. 2012. Comparison of optically derived particle size distributions: Scattering over the full angular range versus diffraction at near forward angles. *Applied Optics* **51**(21): 5085–5099. DOI: http://dx.doi.org/10.1364/AO.51.005085.

**Zhang, X**, **Hu, L**. 2009. Scattering by pure seawater at high salinity. *Optics Express* **17**(15): 12685–12691. DOI: http://dx.doi.org/10.1364/OE.17.012685.

**Zhang, X**, **Hu, L**, **Gray, D**, **Xiong, Y**. 2021. Shape of particle backscattering in the North Pacific Ocean: The $\chi$ factor. *Applied Optics* **60**(5): 1260–1266. DOI: http://dx.doi.org/10.1364/AO.414695.

**Zhang, X**, **Huot, Y**, **Gray, D**, **Sosik, HM**, **Siegel, D**, **Hu, L**, **Xiong, Y**, **Crockford, ET**, **Potvin, G**, **McDonnell, A**, **Roesler, C**. 2023. Particle size distribution at Ocean Station Papa from nanometers to millimeters constrained with intercomparison of seven methods. *Elementa: Science of the Anthropocene* **11**(1): 00094. DOI: http://dx.doi.org/10.1525/elementa.2022.00094.

**Zhang, X**, **Stavn, RH**, **Falster, AU**, **Gray, D**, **Gould, RW Jr.** 2014. New insight into particulate mineral and organic matter in coastal ocean waters through optical inversion. *Estuarine, Coastal and Shelf Science* **149**: 1–12. DOI: http://dx.doi.org/10.1016/j.ecss.2014.06.003.

**Zhang, X**, **Twardowski, M**, **Lewis, M**. 2011. Retrieving composition and sizes of oceanic particle subpopulations from the volume scattering function. *Applied Optics* **50**(9): 1240–1259. DOI: http://dx.doi.org/10.1364/AO.50.001240.

**How to cite this article:** Graff, JR, Nelson, NB, Roca-Martí, M, Romanelli, E, Kramer, SJ, Erickson, Z, Cetinić, I, Buesseler, KO, Passow, U, Zhang, X, Benitez-Nelson, C, Bisson, K, Close, HG, Crockford, T, Fox, J, Halewood, S, Lam, P, Roesler, C, Sweet, J, VerWey, B, Xiong, Y, Siege, DA. 2023. Reconciliation of total particulate organic carbon and nitrogen measurements determined using contrasting methods in the North Pacific Ocean as part of the NASA EXPORTS field campaign. *Elementa: Science of the Anthropocene* 11(1). DOI: https://doi.org/10.1525/elementa.2022.00112

**Domain Editor-in-Chief:** Jody W. Deming, University of Washington, Seattle, WA, USA.

**Guest Editor:** Deborah Steinberg, Virginia Institute of Marine Science, William & Mary, Williamsburg, VA, USA

**Knowledge Domain:** Ocean Science

**Part of an Elementa Special Feature:** Accomplishments from the EXport Processes in the Ocean from RemoTe Sensing (EXPORTS) Field Campaign to the Northeast Pacific Ocean

**Published:** December 1, 2023 **Accepted:** October 9, 2023 **Submitted:** August 25, 2022



ELEMENTA Science of the Anthropocene

*Elem Sci Anth* is a peer-reviewed open access journal published by University of California Press.

OPEN ACCESS